Journal of Chemical, Biological and Physical Sciences

An International Peer Review E-3 Journal of Sciences

*Available online at*www.jcbsc.org

Section A: Chemical Sciences

CODEN (USA): JCBPAT Research Article

Thermodynamic Studies of Depolymerization of Polyethylene Terephthlate (PET) Waste

Vishvanath S. Zope[1*] and Narendra A. Ghule[2]

Department of Chemistry, M.J.College, Jalgaon (M.S.) India,

Department of Chemistry, Shri. V.S.Naik Art's, Commerce and Science College, Raver, Dist: Jalgaon; (M. S.) India

Received: 12 June 2014**; Revised:** 20 July 2014**; Accepted:** 30 July 2014

Abstract: Nowadays the Poly-ethylene terephthalate (PET) is one of the most commonly used synthetic polymers due to the growing application as an engineering plastic. PET waste taken from post-consumer soft drink bottles was subjected to chemical recycling process such as, alkali hydrolysis using sodium hydroxide. Viscosity average molecular weight of The PET waste study was determined by Ostwald method and recorded as 7338. The product obtained in de-polymerization of PET waste is a value added product such as terephthalic acid (TPA). The reactions were studied at different temperature ranging from 373 to 463K and time between 20 to120 minutes. The purified products was characterized by recording its IR and melting point. The velocity constant of depolymerization reaction obtained by measuring the weight of unreacted PET is in the order of 10^{-3} min^{-1}. Thermodynamic parameters such as enthalpy of activation (ΔH), free energy of activation (ΔG) and entropy of activation (ΔS) for sodium hydroxide at 373K were found to be 20.02 $KJmol^{-1}$, $1.63x10^{-3}$ $KJmol^{-1}$and 0.053 $KJmol^{-1}$respectively. Similar thermodynamic study has been carried out for depolymerization reaction with catalysts like lead acetate and pyridine.

Keyword: Alkaline hydrolysis, poly (ethylene terephthalate), Terephthalic acid, Enthalpy of activation (ΔH), Free energy of activation (ΔG), Entropy of activation.

INTRODUCTION

In the last decade, due to worldwide increase in population, the need of people to adopt improved conditions of living led to a drastic increase of consumption of polymer. Worldwide annual consumption of plastic materials has increase from around five million tons in the 1950s to nearly 100 million tons today. The waste plastic creates serious environmental problems. Such problems are solved either by incineration or depolymerization.

Poly (ethylene Terephthalate) (PET) is widely used in the manufacture of high strength fibers, soft drink bottles and photographic film. With increasing PET consumption as packaging material, the effective utilization of PET wastes has received wide attention for the preservation of resources and protection of the environment[1].

The growing interest in PET recycling is due to wide spread use of polyester. A very important characteristics features of PET is that it do not have any side effects on biology of human being, hence it plays a very important role in the manufacture of packaging for food industry. PET does not show a direct hazard to the environment but due to the subsequent fragmentation in plastic waste producing harmful material.

Various chemical processes such as methanolysis, glycolysis, hydrolysis, amminolysis, alkali hydrolysis, acid hydrolysis, and neutral- water hydrolysis are used for chemical recycling of PET waste. Researchers have reported kinetics of alkali hydrolysis for PET[2,3]. Various studies of recycling of PET by acid hydrolysis were reported[4-8].Yoshioka reported the kinetics of hydrolysis of PET in nitric acid with the help of modified shrinking – core model[9].

Alkaline hydrolysis of PET is usually carried out using aqueous solution of KOH and NaOH of the concentration of 11 wt %. This chemical recycling gives a very good result at $200^{O}C$[10].Several researchers has studied the kinetics of neutral hydrolytic de-polymerization of PET[11-15]. In the present work authors have studied the effect of catalyst on alkali hydrolysis of de-polymerization of PET. Lazarus described a process that allows the recovery of terephthalic acid (TPA) from PET waste[16].The kinetics and thermodynamics studies were undertaken to determine the enthalpy of activation, free energy of activation, entropy of reaction and velocity constants of reactions.

EXPERIMENTAL

The PET used in all the experiments was procured from recycled PET mineral bottles. Other materials used were HCl, NaOH, lead acetate, pyridine etc. as it is supplied by S.D. fine chemicals (India). All these chemicals were of analytical grade and used as received.

Determination of molecular weight: The viscosity average molecular weight of PET was determined using Ostwald's viscometer. The flow time of various solutions prepared in solvent phenol and tetrachloroethane 3:5 (v/v) was recorded.

The intrinsic viscosity (intercept =15.9) of the graph $\eta sp / C$ against concentration was used to calculate molecular weight of PET using the formula $[\eta sp / C] = k M^{\alpha}$ where the value of constant k and α for above solvent mixture are 22.9×10^{-3} and 0.73 respectively fig (1). The molecular weight of PET was found to be 7338.

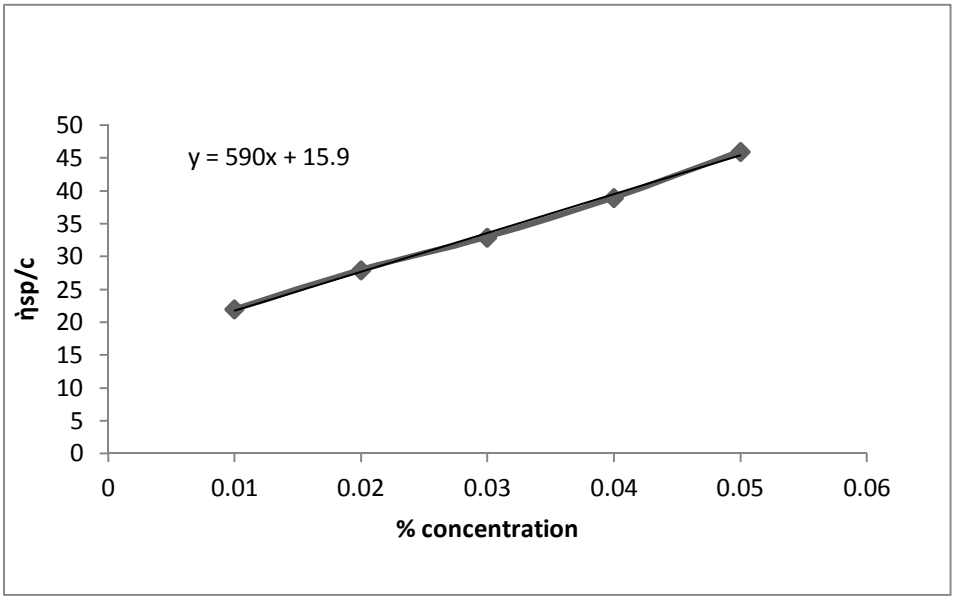

Fig.1: Intrinsic viscosity verses concentration

Alkali hydrolysis of PET using catalyst: Alkali hydrolysis of PET flakes in presence of catalysts were carried out in 250 ml round bottom flask equipped with reflux water condenser heating assembly with magnetic stirrer at 1 atm pressure and temperature ranging from373 to 463K. 6g of PET flakes, 10 g NaOH and 100ml distilled water were charged in the flask. It was reflux for the various time intervals such as 20, 40 60 and 120 minutes. The similar procedures have been carried out using the catalysts such aspyridine and led acetate under the same experimental conditions.

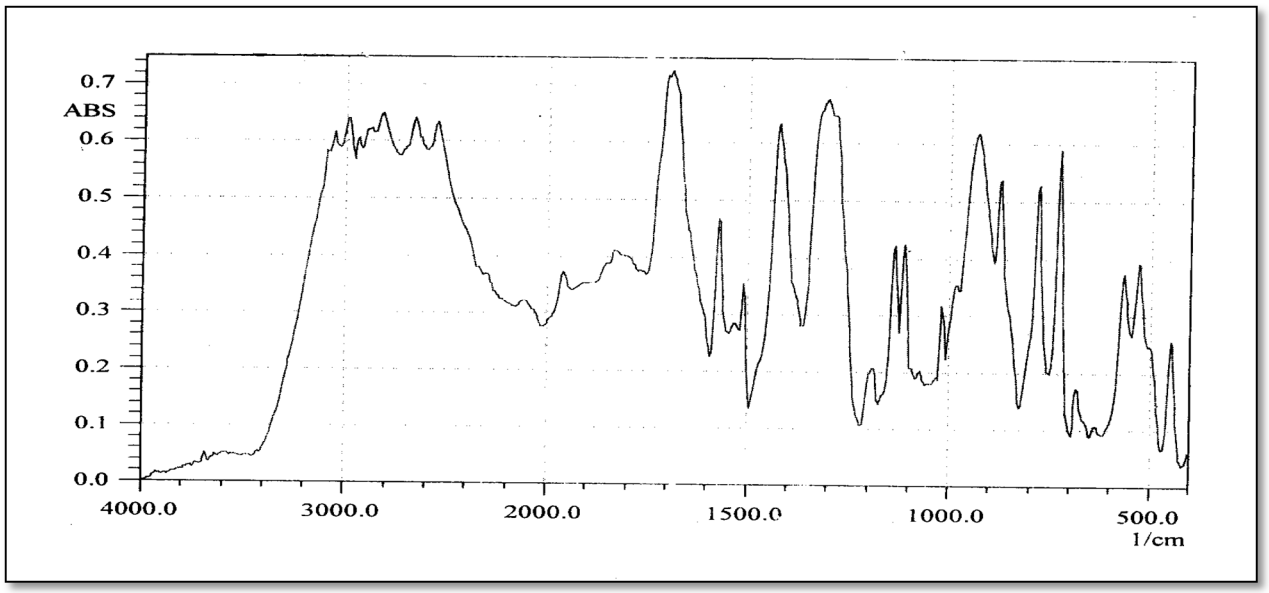

Fig.2: FTIR of TPA of depolymerization of PET

The reaction mixture was filtered for the separation of unreacted PET. The filtrate was treated with concentrated HCl till it become acidic. A white precipitate of pure terephthalic acid (TPA) was obtained which was washed frequently with distilled water till it is completely free from HCl. The filtered white precipitate was dried and weighed. It was characterized by recording its FTIR spectra on a Hyper-IR from Shimadzu (**Fig.2**).

RESULT AND DISCUSSION

Optimization of NaOH and catalyst: Figure 3 to 5 represents the optimization of NaOH, pyridine and lead acetate...

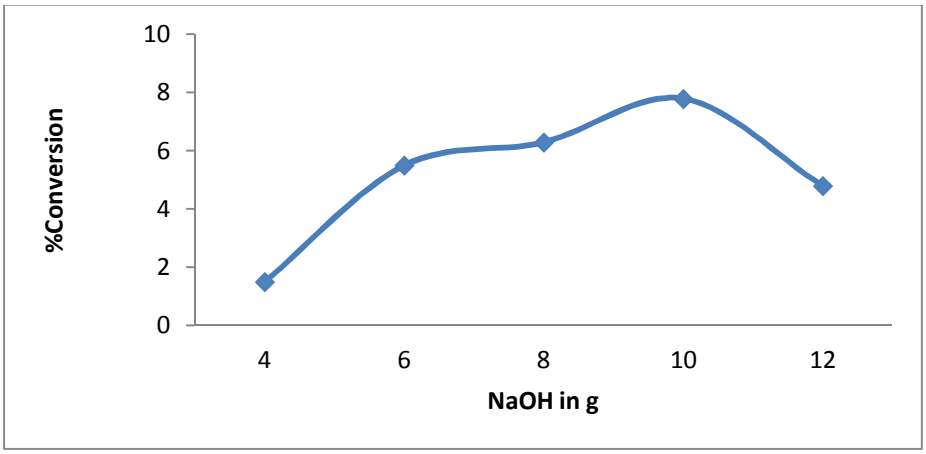

Fig.3: Optimization of NaOH

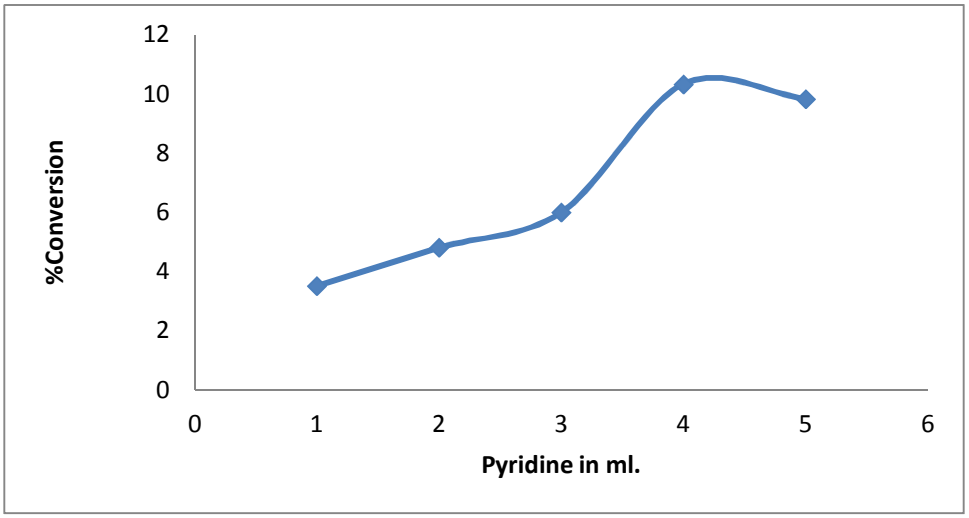

Fig.4: Optimization of pyridine

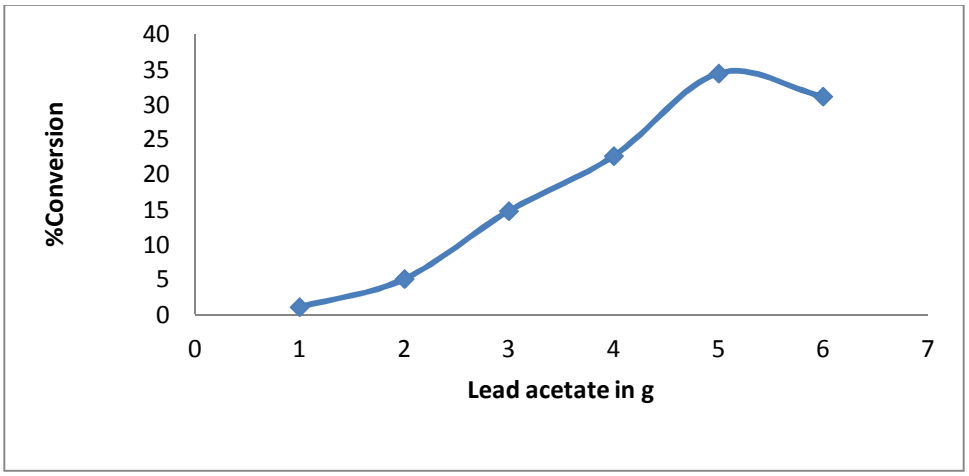

Fig.5: Optimization of lead acetate

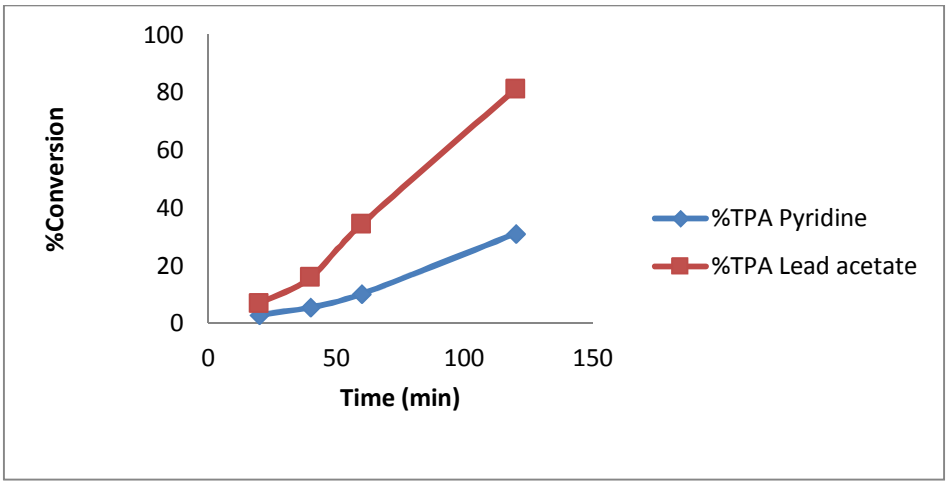

Fig.6: Time verses % concentration

Percent conversion of PET into TPA: Result shows that the percent conversion of PET into TPA increases with increased in reaction time. Figure 6 shows variation of percent conversion of PET into TPA with time. Catalysts accelerate the rate of NaOH hydrolysis for depolymerization of PET.It has been found from the figure that there is gradual increase in percent conversion up to 60 minutes reaction time for both catalysts. Further for lead acetate the percent conversion increases significantly from 34.5% to 81.33% and for pyridine it increases from 10.33% to 31.16%.

KINETICS OF PET DEPOLYMERIZATION

Velocity constant: The kinetics of depolymerization of PET has been studied on the basis of measurements of either weight of TPA obtained or by weight of unreacted PET. The velocity constants of hydrolysis of PET has been calculated using first order equation (1) as:

$$K = \frac{2.303}{t} \log \frac{C_o}{C_t} \quad \ldots (1)$$

Where, C_0 is initial weight of PET in gram

C_t is weight of PET after the reaction time't'.

Energy of activation: The energy of activation of depolymerization PET waste was obtained from Arrhenius plot. The slopes of Arrhenius plot for Sodium hydroxide, pyridine and lead acetate were 2782, 1584 and 2649 (**Fig.7 and 8).** The energies of activation obtained using these slopes were found to be 23.129KJmol^{-1}, 13.169KJmol^{-1} and 22.023 KJmol^{-1} for Sodium hydroxide, pyridine and lead acetate respectively. Hence, the energy of activation decreases by 9.96 and 1.106 KJmol^{-1} using the catalysts pyridine and lead acetate respectively. Decrease in energy of activation for the catalysts indicates that less energy is required for the depolymerization reactions. Hence pyridine is found to be a best suitable catalyst as compare to lead acetate.

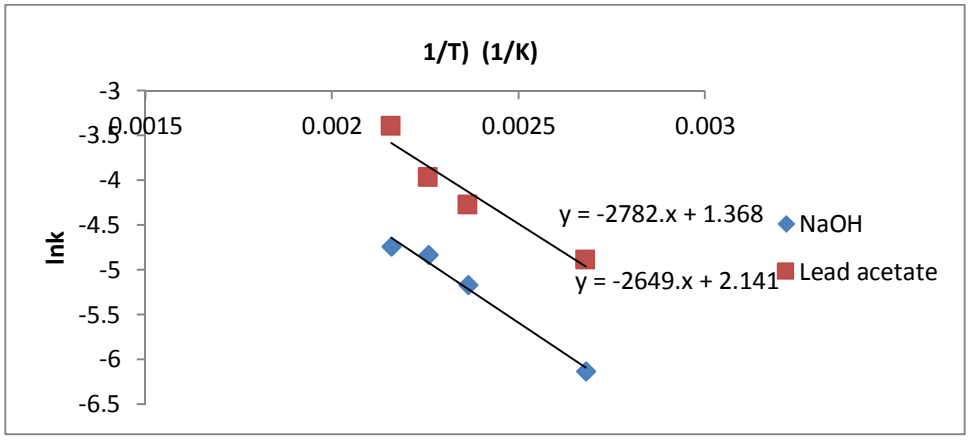

Fig.7: 1/T verses link for Lead acetate

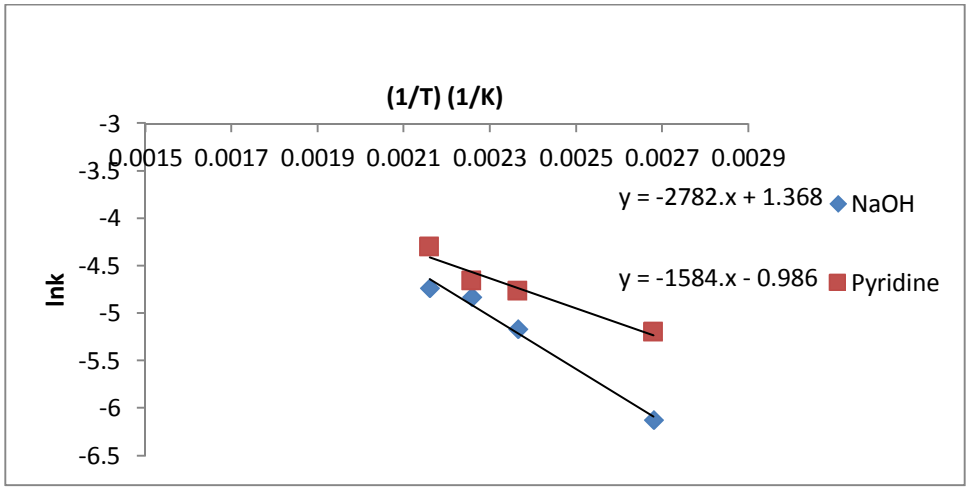

Fig.8: 1/T verses lnk for Pyridine

The frequency factors for sodium hydroxide, lead acetate and pyridine were 0.2456, 0.1175 and 0.3690 obtained by the intercepts of the Arrhenius plots. The higher value of frequency factor for pyridine

indicates maximum collision between the reactants which leads to greater yield of TPA as compare to the reaction without catalysts.

Thermodynamic of PET depolymerization: Enthalpy of activation (ΔH) at specific temperatures using the values of energy of activation is calculated by the equation (2)[17].

$$\Delta H = Ea - RT \quad \ldots (2)$$

Where, R is molar gas constant and T is temperature in Kelvin.

It is evident from the **Table (1),** as temperature increases from 373K to 463K, enthalpy of activation in case of NaOH decreases from 20.02 to 19.27 $KJmol^{-1}$. Similar trends have been observed in case of depolymerization with catalysts.

Table-1: Thermodynamic parameters; ΔH, ΔS and ΔG

Temp (K)	Enthalpy of activation (ΔH) $KJmol^{-1}$			Entropy of activation (ΔS) $KJmol^{-1}$			Gibbs free energy of activation (ΔG) x 10^{-3} $KJmol^{-1}$		
	NaOH	Lead acetate	Pyridine	NaOH	Lead acetate	Pyridine	NaOH	Lead acetate	Pyridine
373	20.02	18.92	9.5248	0.0536	0.0507	0.00255	1.63	-0.29	1.31
423	19.61	18.50	9.1091	0.0463	0.0437	0.00215	1.72	3.98	1.81
443	19.44	18.34	8.9428	0.0438	0.0414	0.00201	1.73	-0.2	3.15
463	19.27	18.17	8.7766	0.0416	0.0392	0.00189	-0.32	1.25	2.15

It is interesting to note that decrement in the values of enthalpy of activation has found to be significant for pyridine as compare to lead acetate. Unlike enthalpy of activation, entropy of activation and energy of activation the free energy of activation for various temperatures for NaOH was found to be nearly equal to one. Similar results were found for the catalyst.

The entropy of activation at specific temperature using value of energy of activation is calculated by the equation (3)[17].

$$e^{\Delta S/R} = h/kT\ (k_1\, e^{\Delta H/RT}) \quad \ldots(3)$$

Where, ΔS is entropy of activation, R is molar gas constant, h is Plancks constant, T is temerature in kelvin, k is Boltzman constant, k_1 is velocity constant and ΔH is enthalpy of activation. It has been found that the entropy of activation for NaOH decreases from 53.69$Jmol^{-1}$ to 41.60 $Jmol^{-1}$ as temperature incrases from 373 to 463 K. Similar trends for entropy of activation have been observed in case of pyridine and lead acetate.It is evidend from this trend that rise in entropy of activation is due to disordernees of the system.In case of pyridine the decrement in entropy of activation is significant as compare to the lead acetate and without catalyst. Hence as mentioned above pyridine has been found to be a best suitable catalyst in the light of entropy of activation data.

CONCLUSIONS

The following conclusions were drawn

1. Viscosity average molecular weight of PET waste bottle was found to be 7338.
2. The energy of activation (13.169 $KJmol^{-1}$) and frequency factor (0.3690 min^{-1}) shows requirement of less amount of energy for depolymerization of PET using pyridine as catalyst.
3. Change in enthalpy (ΔH) and entropy (ΔG) decreases with an increase in temperature.
4. Depolymerization of PET is gradually increases up to 60 minutes, further there is significant increase in percent conversion for depolymerization with and without catalysts.

REFERENCES

1. M.Ghaemy, K.Mossaddegh; Depolymerization of poly (ethyiene terephthalate) fibre wastes using ethylene glycol. *Polymer Degradation and Stability*, 2005, 90,570-576.
2. S.Mishra S.V. Zope, A.S. Goje. Kinetics and thermodynamic study of poly (ethylene terephthalate Waste by saponification reactions. *Polymer international*, 2002, 51(12), 1310.
3. S.Mishra A. S., Goje V. S., Zope , Plastic Waste Management and Environment, New Delhi, India, March,2001 15, 163.
4. D.S.Ravens, The chemical reactivity of Poly (ethylene terephthalate): Heterogeneous Hydrolysis by Hydrochloric Acid, Polymer (London), 1960, 1, 375.
5. T.Davies, P.L. Goldsmith D.A., Ravens I.M, Ward, The kinetics of the hydrolysis of Poly (ethylene terephthalate) Film. *J. Phys. Chem.,* 1962, 66, 175.
6. G.E.Brown R.C., Obrien , Method for recovering Terephthalic Acid and Ethylene Glycol from Polyester materials, U. S. Patent,1976, 3, 952, 053.
7. S.F.Pusztaseri, Method for recovery of Terephthalic Acid from polyester scrap. U. S. Patent. 1982, 4, 355, 175.
8. Toshiaki Yoshioka, Tsutomu Motoki, and AkistsuguOkuwakis. Kinetics of hydrolysis of Poly (ethylene terephthalate) powder in Sulphuric Acid by a modified shrinking – core Model. *Ind. Eng. Chem. Re*s., 2001, 40, 75-79.
9. T.Yashinka, T. Mtoki, A. Okuwaki, *Ind.Eng. Chem. Res*. 2001, 40, 75.
10. S.Baliga, W.T. Wong, *J.Polym Sci*, Part A: *Polym.Chem*, 1989, 27, 2071.
11. J.R.Campanelli, M. R. Kamal, D.G. Cooper, J. *Appl. Polym. Sci*.1993, 48, 443.
12. J.R.Campanelli, D.G., Cooper, M.R., Kamal, J. *Appl Polym Sci*, 1994, 53, 985.
13. A.Launay, F.Thominetted Verdu*, J. Polym Degrad Stab*, 1999, 63,385.
14. S.Weidner, G. Kuehn, B.Werthmann, H. Schroeder U. Just R. Borowski,B. Decker,B. Schwarz, Schmuecking, I. Seifert , *J. Polym .Chem,*1997, 35, 2183.
15. C.Y.Kao, W.H. Cheng, B.Z. Wan, *Ind. Eng .Chem. Res*, 1998, 37, 1228.
16. S.D.Lazarus J.C., Twilley, O.E.Snider, 1967, US Patent,1967, 3,317,519.
17. K.J Laidler. Chemical kinetics 2nd Edn, Dirling Kindersley (India) Pvt.Ltd., Pearson Education in South Asia, New Delhi (India)2007,. 114.

*** Corresponding author:** Vishvanath**;**
Department of Chemistry, M.J.College, Jalgaon (M.S.) India,

International Journal of Advanced Research in Chemical Science (IJARCS)
Volume 2, Issue 2, February 2015, PP 1-7
ISSN 2349-039X (Print) & ISSN 2349-0403 (Online)
www.arcjournals.org

Catalytic Depolymerization of Polyurethene Using Zinc and Lead

Vishvanath S. Zope

Department of Chemistry
M. J. College, Jalgaon, (MS)
dr_zope@rediffmail.com

Abstract: *Neutral hydrolytic depolymerization of the Polyurethane (PU) Foam waste was done using 0.5 L high pressure autoclave at temperatures of 150^0,180^0,200^0 and 240^0 C, the autogenious pressures of 75, 160, 220 and 480 psi and time intervals of 30, 45, 60 and 90 minutes. Extent of depolymerization of polyurathene was studied by measuring the amine value of the product. Optimum amount of catalysts such as zinc acetate and lead acetate was found to be 1g. Zinc acetate was more effective catalyst than lead acetate for the depolymerization of PU foam reaction. On the basis of amine value and residual weight of the depolymerized product, the velocity constant was obtained and found to be in order of 10^{-3} min^{-1}; and the reaction was found to be first order. The energy of activation and frequency factor obtained by Arrhenius plot were 36.86 kJ mole $^{-1}$ and 1.349 x 10^2 min^{-1} respectively. The enthalpy of activation at 150^0C, 180^0C, 200^0C, and 240^0C was recorded as 43.89, 44.39, 44.72 and 45.37 $kJmole^{-1}$ respectively. The entropy of activation at the respective temperatures was recorded as 10.37 x 10^{-2}, 9.79 x 10^{-2}, 9.45 x 10^{-2} and 8.84 x 10^{-2} kJ $mole^{-1}$.*

Keywords: *Energy of Activation, Depolymerization, Kinetics, Free Energy of Activation*

1. INTRODUCTION

Hydrolysis, glycolysis and aminolysis are well known processes used for depolymerization of PU in to amines and polyols. Polyurethane on hydrolysis produces primary polyols, carbon dioxide and the amine of conjugate isocynate. Depolymerization of PU foam by alcoholysis uses alcohol as the cracking agent. Alcoholysis and hydrolysis proceed in similar way, having slight difference in chemical reaction. Different rout is responsible for getting entirely different products. As polyurethane production increases, the amount of PU waste also increases. Traditional methods of destroying this waste are not particularly acceptable. Burning of polyurethane waste sends oxides of nitrogen, hydrocyanic acid, carbon dioxide and other toxic compounds in the atmosphere. When it is buried, it is broken down by action of water to give urea. This process causes pollution of air and water in environment. The most effective method of polyurethane waste processing is glycolysis, based on thermo-chemical interaction between polyurethane and hydroxyl containing compounds[1-2]. Literature survey indicates, glycolysis process can be used to resolve the disposal problems of PU waste and with obtaining high quality of polyols. Kouji et al[3] have indicated the method to design a comfort path of PU recycling. The degradation of polyurethane foam was carried out with diethylene glycol as a solvent and sodium hydroxide as the catalyst[4]. In the present work PU waste was depolymerized by neutral hydrolytic process in presence of zinc acetate and lead acetate as catalysts. The amount of catalyst was optimized.

2. EXPERIMENTAL

5 g PU foam, 300 ml water and catalyst of definite amount were charged in the reaction vessel. The reaction was carried out for 60 minutes at temperature 180^0C by varying the amount of catalysts from 0.4-1.2 g. Further the reaction was carried out using optimized amount of catalyst by varying the temperature from 150^0, 180^0, 200^0 and 240^0 C for the reaction time of 30, 45, 60 and 90 minutes. After the specified reaction time the vessel was cooled suddenly by circulating cold water through the inner coil. The vessel was opened by removing collar of reactor of high-pressure autoclave. Obtained product was cooled to room temperature. The reactant was filtered using Whatman filter paper. Amine values were determined using one gram of depolymerized

product by AOCS method

$$\text{Amine value} = \frac{\text{Equivalence point x N x 56.1}}{\text{W}}$$

W = Weight of sample in gram.

N = Exact Normality of HCl

The depolymerized product was taken for recovery of value added product. It was recovered by adding potassium hydroxide into depolymerized product. The recovered salt was characterized by recording FTIR spectra on Hyper FTIR of SHIMANDZU make.

3. RESULTS AND DISCUSSION

3.1. Optimization of Catalysts Concentration for Depolymerization of PU Foam

Depolymerization of PU foam waste was studied using lead acetate and zinc acetate as catalysts. Both the catalysts were taken from 0.4 g to 1.2 g using, 5 g of PU foam waste in 300 ml water at temperature of 180^0C and autogenious pressure of 160 psi for reaction time of 60 minutes. Results show an increase in percent conversion of PU foam waste with increase in amount of the catalysts,100% and 71% PU foam was found to be depolymerized by taking 1g of zinc acetate and lead acetate respectively. Further increase in amount of catalyst results decrease in percent conversion in case of lead acetate (Figure 1). Hence the optimized amount of catalyst for the depolymerization reaction is found to be 1 g for both zinc acetate and lead acetate. Decrease in percent conversion beyond optimized amount is might be due to occurring of reverse reaction at higher concentration of catalyst.

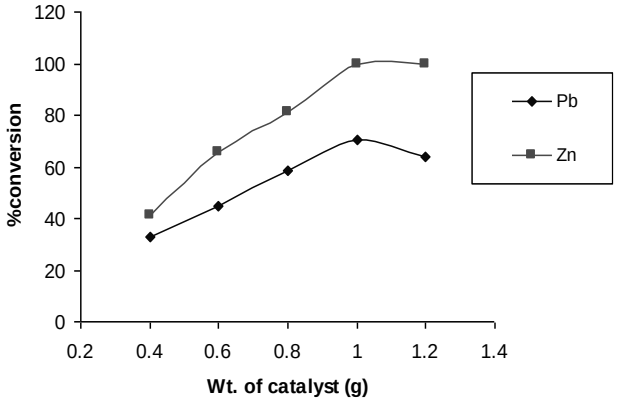

Fig1. *Depolymerization of PU foam waste with catalysts at180^0 C and 160 psi autogenious pressure for the reaction time 60 minutes.*

To measure the depolymerization value of PU foam waste, amine value of depolymerized product was determined (Figure 2). Behavior of the figure 2 is exactly same as that of figure 1. It shows an increase in amine value with increase in concentration of catalyst up to 1g and thereafter there is slight decrease in amine value for both the catalysts. It is also evident from this figure that the optimum weight of catalyst for depolymerization of 5 g PU foam waste is 1 g.

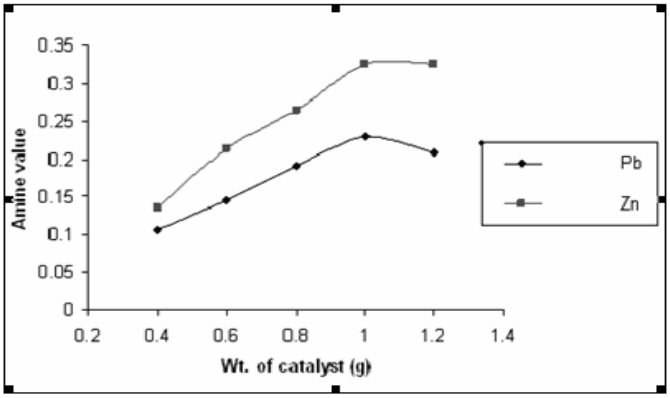

Fig2. *Effect of catalyst on depolymerization of PU foam waste at 180^0C by measuring the amine value.*

Figure 3 shows the results of amine values of depolymerized PU foam with increasing reaction time from 30 minute to 90 minute at 1 g of optimized amount of catalyst at 180^0C temperature and at autogenious pressure of 160 psi . The amine values increase with increase in time from 30-90 minute of reaction time in case of zinc acetate and uncatalysed reaction. The increments in amine value are recorded as 0.2246 for 30 minute reaction time and 0.3358 for 90 minute reaction time for zinc acetate. These values are highest for respective reaction times of lead acetate and uncatalysed reactions. It is worthy to mention that the lead acetate shows increase in amine value up to 0.3011 for 60 minute and thereafter it decreases to 0.2884 for 90 minutes of the reaction time. But it is also evident that zinc acetate catalyst is an effective catalyst for the depolymerization of PU foam waste, as the amine value is always greater at any instant as compared to that of lead acetate and without catalyst. Hence in this study we have undertaken the optimized amount (1 g) of zinc acetate catalyst for all the depolymerization reactions.

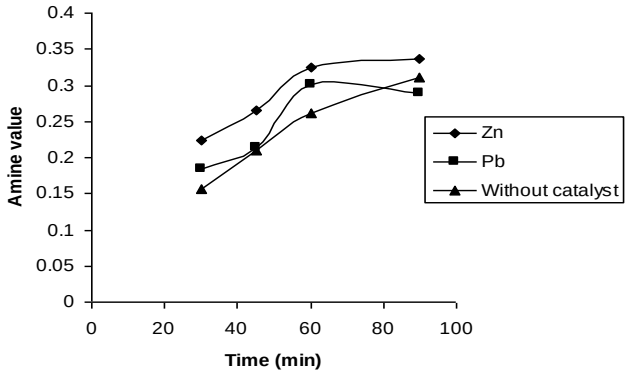

Fig3. *Effect of reaction time on depolymerization of PU foam waste with and without catalysts at 180^0C reaction temperature.*

3.2. Kinetics of Depolymerization of PU Foam Waste

PU foam on depolymerization breaks into fragments of NCO groups. The rate of depolymerization depends on number of NCO groups produced.

The NCO-groups produced in depolymerization reaction react with water to form amine; hence, rate of depolymerization is decided by measuring amine value at various time intervals.

The mechanism of the reaction can be represented as,

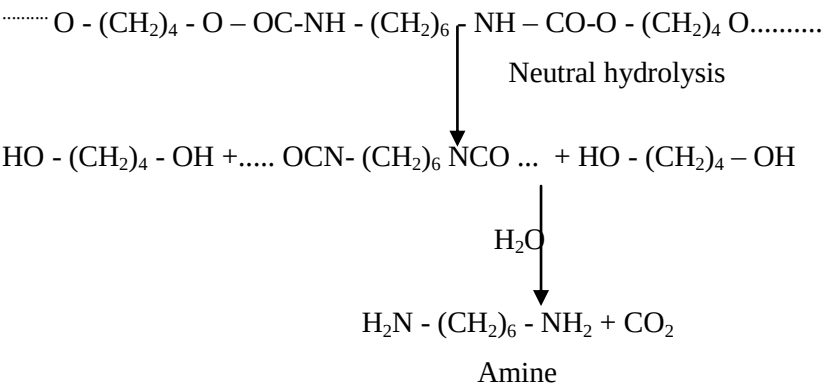

The rate of depolymerization was determined by measuring the amine value of the reaction product as well as residual weight of the PU foam waste. Amine value at zero time measures amine groups available at zero time. Similarly the amine value at $t = \infty$ is a measurement of total amine groups present after the completion of reaction. The first order kinetic model proposed by auothers[5] was found to be fit for our study using different catalyst,

$$k = 1/ t [- \ell n (1\text{-Amine value})] \quad (1)$$

Equation (1) was used to calculate the velocity constant of depolymerization of PU foam on the basis of measurement of amine value. The values obtained for velocity constant at temperature 180^0C and at autogenious pressures of 160 psi were plotted against the weight of the catalysts. Figure 4 shows velocity constants, which are obtained maximum (6.56×10^{-3} and 4.36×10^{-3} for

zinc acetate and lead acetate respectively) for 1 g of the catalysts. The values of velocity constants are recorded as 6.56 x10 $^{-3}$ and 3.88 x10^{-3} for zinc acetate and lead acetate at 1.2 g of catalysts. Thus it can be concluded that below optimum amount of the catalysts the reaction is slow in case of both the catalysts, and above the optimum amount the reverse reaction is there in case of lead acetate.

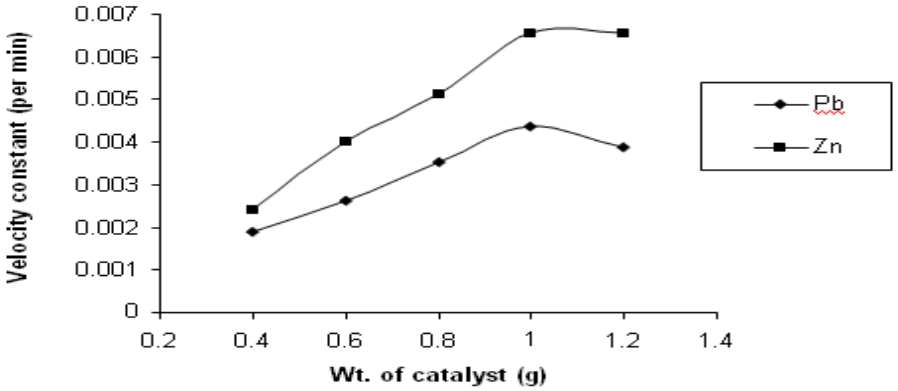

Fig4. *Effect of amount of catalyst on velocity constants (min $^{-1}$) for depolymerization of PU foam waste at 180^{0}C*

Velocity constants of the depolymerization reactions are also determined by using residual weight left after the complete reaction by equation as given below,

$$k = \frac{2.303}{t} \log \frac{C_o}{C_t} \quad (2)$$

Where $[C]_O$ is the concentration of the reactant at time t = 0 and $[C]_t$ is the concentration of the reactant at time t. It is observed that the velocity constants obtained by equation (1) and (2) are identical and are of the order of 10^{-3} min.$^{-1}$

Figure 5 shows an increment in the velocity constant with temperature at all the time intervals. An increase in velocity constants of the reactions is due to higher kinetic energy of the molecule obtained by thermal agitation. However, as reaction time increases the velocity constant decreases. The velocity constants increase for the 30 minutes reaction time but subsequently, at 45, 60 and 90 minutes, these values decrease successively for all respective temperatures, since the product of the reaction was not removed. It might be due to a Le-Chatelier effect [6].

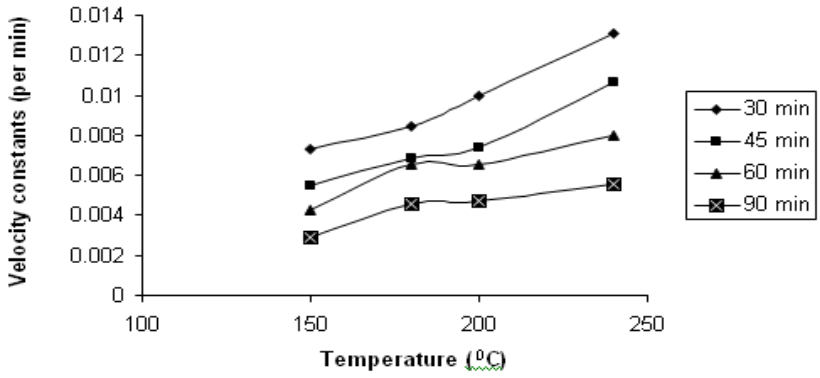

Fig5. *Effect of temperatures on velocity constants at different reaction time interval using optimized zinc acetate catalyst.*

The amine value at 150^0 C remains almost constant (0.22) at various time intervals. Figure (6). While variation in amine value increases up to 0.32 with time at 180^0 C and 200^0 C. Further the amine values remain almost constant at these temperatures. The degree of depolymerization is significant at 240^0 C. Initially up till 45 minutes reaction time, amine value gradually increases to 0.38 and thereafter it remains constant.

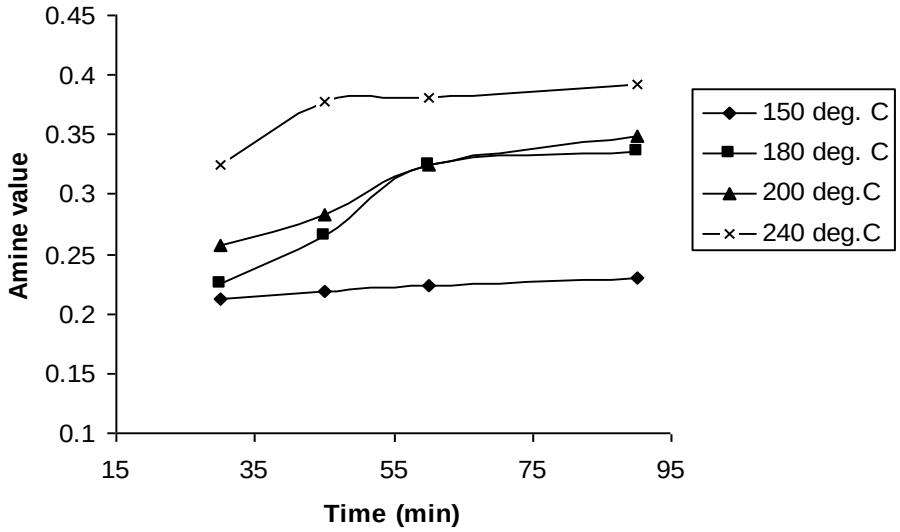

Fig6. *Effect of reaction time for depolymerization on amine value at different temperatures using optimized zinc acetate catalyst*

As per the reaction mechanism shown earlier, each chain scission utilizes one water molecule to form one each of amine and glycol end groups. Therefore, the progress of the reaction was studied by measuring concentrations of amine groups after the definite reaction time.

The rate of amine end group formation may be expressed as ,

$$d[-NH_2] / dt = k [PU][water] – k' [-NH_2] [OH] \quad (3)$$

Therefore, the equilibrium constant Ke is given as,

$$Ke= k / k' \quad (4)$$

Where, k = the rate constant of forward reaction (depolymerization),

k' = the rate of reverse reaction (condensation),

[PU] = concentration of polyurethane foam,

[Water] = concentration of water,

$[-NH_2]$ = concentration of amine end group,

[OH] = concentration of hydroxyl end group

Equations 4 was used to calculate rate constant of reverse reaction and hence the equilibrium constants were determined.The results of comparative study of velocity constants with and without catalyst of depolymerization reaction at temperatures 100^0,150^0, 180^0,200^0,and 240^0 C and at autogenious pressure were studied by Mishra et al[6]. The values of velocity constants obtained by measuring residual weight and amine values were found to be identical and these are in order of 10^{-3} min^{-1} . It indicates that the mathematical first order kinetics model proposed by Mishra et al[6] is justified.

3.3. Thermodynamics of Depolymerization of PU Foam Waste

Arrhenius plot was used to elucidate the activation energy. The energy of activation for depolymerization of PU foam waste was obtained by studying the depolymerization reaction at the temperatures ranging from 150^0 C to 240^0 C. The Arrhenius plot was drawn using the values of ln k versus 1/T. The slope of Arrhenius plot was found to be 4433.6 unit which was used to calculate the energy of activation. The energy of activation for depolymerization of PU foam waste was calculated as 36.86 kJ $mole^{-1}$ (Figure 7). The intercept of Arrhenius plot is 4.9046 units, which is used to determine the frequency factor of the reaction, and it is found to be $1.349x10^2$ min^{-1}. It shows that reactant molecules collide with each other with the frequency $1.349x10^2$ min^{-1}.

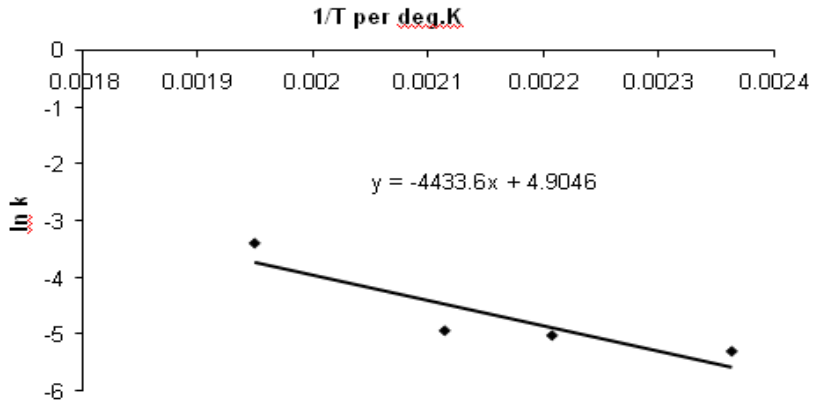

Fig7. *Arrhenius plot of variation of velocity constant (ln k) versus reciprocal of absolute temperature (1/T)*

4. CONCLUSION

The enthalpy of activation at various temperatures was obtained using the equation[7] [redacted] = E_a + 2RT. The minimum value of [redacted] (43.89 kJ mole^{-1}) was recorded for 150^{0}C reaction temperature, while maximum (45.37 kJ mole^{-1}) for 240^0 C; on recording the entropy, the values are vice versa. It is evident from the values that as temperature increases, enthalpy of activation increases while entropy of activation decreases. The decrease in entropy with increase in temperature is due to higher rate of depolymerization so that conversion of PU foam waste obtained at early time.

Kinetic and thermodynamic parameters such as velocity constant for forward reaction (k), velocity constant for reverse reaction (k'), thermodynamic equilibrium constant (Ke) and Gibbs free energy (ΔG) at temperature 180^{0}C and for 60 minutes reaction time are summarized in Table1. Results show that as the amount of the catalyst increases the Gibbs free energy of activation also increases up to 1 g of catalyst. Hence this amount is an optimum amount for depolymerization of PU foam waste. Same behavior is observed for zinc acetate catalyst, however the values of k, k'and ΔG can not be evaluated since residual weight was not available due to complete disappearance of the reactant. However in case of lead acetate, the value of Ke is recorded in decreasing order from 32.38 to 5.99 for 0.4 to 1.0 g .Thereafter the value of Ke increases up to 7.58 for 1.2 g of lead acetate catalyst. Likewise value of ΔG increases up to 1 g of catalyst and further decreases for 1.2 g of lead acetate. Thus it is concluded that reversible reaction becomes more pronounced beyond 1 g of lead acetate as catalyst.

Table1. *Kinetic and Thermodynamic parameters for depolymerization of PU foam waste at 180^0 C using different catalysts*.

Weight (g)	Lead acetate catalyst				Zinc acetate catalyst			
	k x10^{-3} min^{-1}	k ' x10^{-4} min^{-1}	Ke	-Δ G kJ mole^{-1}	k x10^{-3} min^{-1}	k ' x10^{-4} min^{-1}	Ke	-ΔG kJ mole^{-1}
0.4	1.878	0.57	32.38	13.097	2.71	1.393	19.45	11.177
0.6	2.627	1.572	16.71	10.605	4.31	6.019	7.16	7.413
0.8	3.527	3.799	9.28	8.390	5.316	11.210	4.38	5.562
1.0	4.356	7.262	5.998	6.746	-	-	-	-
1.2	3.878	5.110	7.586	7.631	-	-	-	-

REFERENCES

[1]. Lubartovich SA, Morozol Yul, Tretiakov OB., Polyurethane formation reaction, Kimiia Moscow, 1990

[2]. Happer JFG, Parrinello G, Parfondary A., Recent development in chemical recycling of flexible polyurethanes, UTECH-92 Conf.The Hague, Netherland, 1992

[3]. Kouji K and Shizuo T., Decomposition of polyurethane foams by alkanolamines, J. Appl. Polym. Sci., **51**, 675-682, 1994

[4]. Mir Mohammad Alavi Nikje, Moslem Haghshenas, Amir Bagheri Garmarudi Polymer Bulletin, Preparation and application of glycolysed polyurethane integral skin foams

recyclate from automotive wastes**, 56**, 257-265, 2006

[5]. and Kulkarni RD., Kinetics and Thermodynamics of Hydrolytic Depolymerization of Polyurethane foam at higher temperatures and pressure, Polym Plastics Tech and Engg. **43**, 1001-1011, 2004

[6]. Mishra S, Zope V. S., First order kinetic model of depolymerization of polyurethane foam Orient.J.Chem, 19: 589-594, 2003

[7]. Laidler KJ, Chemical Kinetics, Second Edn, Dirling Kindersley (India) Pvt.Ltd.,Pearson Education in South Asia, New Delhi (India); 114, 2007

AUTHOR'S BIOGRAPHY

Dr. V. S. Zope is Associate professor in chemistry at M. J. College, Jalgaon. He has 27 year experience in teaching and 20 years in research. He has completed his doctorate degree from North Maharashtra University, Jalgaon in the subject of Chemical Recycling of Plastic Waste in the year 2004. He has to his credit 26 publications in National and International research journal of repute. 01 student has awarded Ph.D. and 02 were awarded M. Phil. under his guidance and at present one student is doing Ph. D. He was the chairman of steering committee for NAAC re-accreditation process of the college which is awarded as "A" grade with highest CGPA score of 3.63 at 4 point scale. He is the author of 26 text books in physical and analytical chemistry useful especially for the students of under graduate. He visited Thailand, Malaysia, Estonia, Denmark, Finland, Norway, Estonia and Sweden to attend and present research papers in conferences and study the educational systems of abroad.

Available online at www.derpharmachemica.com

ISSN 0975-413X
CODEN (USA): PCHHAX

Der Pharma Chemica, 2016, 8(21):1-5
(http://www.derpharmachemica.com/archive.html)

Gold Nanoparticles Catalyzed Synthesis of Ibuprofen Intermediate in Aqueous Ethanol

Sandeep J Pawar[1], Shivkumar Y Patil[1], Pramod P Mahulikar[1] and Vishwanath S Zope[2]*

[1]*School of Chemical Sciences, North Maharashtra University, Jalgaon 425 001, MS, India*
[2]*Department of Chemistry, Moolji Jaitha College, Jalgaon 425001, MS, India*

ABSTRACT

Ibuprofen was globally consumed drug in huge quantity. It was industrially synthesized by traditional process which generates more waste and used hazardous organic solvents. Hence, it is need to develop environmental benign catalytic synthesis of ibuprofen. We synthesized pearl necklace shaped gold nanostructured material with diameter about 4 nm. Gold nanoparticles (AuNPs) were prepared and tested for the activity in the catalytic reduction of 4-nitrophenol (4-NP) to 4-aminophenol (4-AP) showed excellent catalytic performance. Further, using AuNPs we catalytically synthesized 1-(4-isobutylphenyl)ethanol which is important drug intermediate for the widely used Ibuprofen. The rate constants was determined at room temperature 0.167 ± 0.003 per minute. The recyclability study of AuNPs in the reduction of 1-(4-isobutylphenyl)ethanone (IBPEON) to 1-(4-isobutylphenyl)ethanol (IBPE) in six consecutive reaction cycles found to be (92%), (89%), (86%), (85%), (81%), (77%), respectively. We emphasized, the reported synthesis was smoothly performed in the mild reaction conditions under environmentally benign alternative.

Keywords: Gold nanoparticles, Activation energy, Recyclability, Ibuprofen, 1-(4-isobutylphenyl) ethanol

INTRODUCTION

In the sustainable chemistry of nanoscience and nanotechnology, noble metal nanoparticles have played an important role in the catalytic synthesis of pharmaceutical drugs. Nanotechnology is applicable to most field of science like pharmaceuticals drugs, organic synthesis and is the current focus of researchers. Noble metal particles such as Ag, Pt, Au and Pd have been widely used for catalytic reactions in current research. Gold nanostructured materials have recently gained attention as heterogeneous catalyst in the reduction reactions due to their unique properties like high surface area towards small particle size, high catalytic activity and efficiency to afford high yield of product [1]. AuNPs widely synthesised by several methods including chemical reduction method [2-3], photochemical method using UV [4,5], sonochemical [6,7], biochemical reduction method [8,9], seed-mediated growth method [10,11] and sono-electrochemical method [12,13] etc. Amongst these methods, chemical reduction method is the most easy, safe and clean method for the synthesis of AuNPs. Due to high surface area AuNPs widely used as catalyst in many organic transformations included hydrogenation [14,15], cross coupling reactions [16,17], oxidation [18,19], electron transfer reactions [20].

Nanostructured materials widely used as catalyst is of interest since, catalysis has developed into important technologies in the petroleum, fine chemicals, bulk chemicals and pharmaceutical industries [21]. 1-(4-isobutylphenyl)ehanol (IBPE) is one of the most important drug intermediate used for the synthesis of non-steroidal anti-inflammatory drug (NSAID) Ibuprofen. In the synthesis of 1-(4-isobutylphenyl) ethanol traditionally used hazardous organic solvents [22]. Hence, it is need to develop environmentally benign process for the synthesis of ibuprofen which has very hugely consumed globally.

In the present investigation, we have synthesised spherical necklace shaped AuNPs by chemical reduction method using sodium borhydride. The synthesised AuNPs were tested for determined catalytic activities using the model reaction of the conversion of 4-nitrophenol (4-NP) to 4-aminophenol (4-AP) [23,24]. Further, we used synthesised AuNPs as a catalyst in the synthesis of ibuprofen intermediate 1-(4-isobutylphenyl) ethanol (IBPE) from 1-(4-isobutylphenyl) ethanone (IBPEON) using environmental

benign solvent (Scheme 1). We promisingly not even report benign synthesis of ibuprofen intermediate also proved the six times consecutively recycled AuNPs with high yield of drug against poisoning of catalyst. Also, the reaction was completed within 10 minutes at room temperature.

MATERIALS AND METHODS

Chemicals

All chemicals (4-nitrophenol ($C_6H_5NO_3$, 99%), sodium borohydride ($NaBH_4$, 99%), gold nitrate, ($HAuCl_4$ 50% Au basis) 1-(4-isobutylphenyl) ethanone ($C_{12}H_{16}O$, 98%) and deionized water from Milli-Q system) were purchased from Sigma-Aldrich or Spectrochem or HiMedia and used as received.

Characterizations

The characterizations of AuNPs were collected from various instrumental techniques. The UV-Visible absorption measurement was performed on Shimadzu UV 1800 Spectrophotometer. Water as blank and reference. Transmission electron microscopy was performed on a Philips CM-200 TEM operating at 200 kV, by depositing 20 µL of dispersed sample onto a 300 mesh copper grid coated with carbon layer IR spectra were collected at room temperature from Shimadzu FTIR-Affinity-1instrument in dried KBr pellets in the range 4000 to 400 cm^{-1}. Mass spectra (MS) of 1-(4-isobutylphenyl)ethanol was collected from WATERS, Q-TOF MICROMASS (LC-MS) instrument.

Synthesis of silver nanoparticles (AuNPs)

The AuNPs were synthesized by using chemical reduction method. In brief, 10 mL of 1×10^{-3} M $AgNO_3$ taken in 50 ml of beaker and kept on magnetic stirrer. Then freshly prepared ice cold 30 mL solution of 2×10^{-3} M $NaBH_4$ was hastily added into $AgNO_3$ with vigorous stirring in which the colour change from black to orange and finally pale yellow was observed. Then AuNPs solution was stirred for four hours for good stability and prepared nano-size of AuNPs nanostructured materials. Finally, prepared AuNPs were kept overnight to remove excess hydrogen and used as a catalyst in the model after their characterization.

Typical procedure for catalytic reduction of 4-nitrophenol (4-NP)

The heterogeneous catalytic reduction of 4-NP was performed at room temperature in air. In this typical reaction 1.0 mL of 5×10^{-2} M $NaBH_4$ and 10 µL of AuNPs were mixed for two minutes in 3.0 mL quartz cuvette. To this mixture 1.5 mL of 1×10^{-4} M PNP was added and mixed. The reaction was followed by observing the absorbance spectrum of 4-NP at λ 400 nm. The 4-NP spectrum diminished at every one minute time interval and new spectrum was observed at λ 300 nm is indicates that formation of new product, which was confirmed by isosbestic points [25]. These results were in good agreements with reported literatures [26]. The absorbance spectra were recorded within the wavelength range of 250 – 600 nm. Further, the same experiment were also performed in the temperature range of 298 – 323 K to determine the effect of temperature on the Pseudo first-order rate constant.

Synthesis of 1-(4-isobutylphenyl) ethanol (IBPE)

Aqueous ethanol (3.0 mL) was added in 3.0 mL of AuNPs in round bottom flask, kept in ice bath with constant stirring. This mixture we named as "Alcoholic AuNPs". In the mixture 0.43 g of $NaBH_4$ was slowly added and finally 1.0 g. of IBPEON added with constant stirring. After complete addition, the reaction mixture was removed from the ice bath and stirring was continued at room temperature. The reaction was completed within 5 to 10 minutes and it was preliminary confirmed by thin layer chromatography (TLC). The product was isolated using ethyl acetate as organic layer and AuNPs remained in alcoholic layer. The solvent was removed by rotary evaporator and product was dried at room temperature.

Recycling studies

The recycling study of AuNPs were reported so far, for the catalytic reduction of 4-NP to 4-AP. The above (4-NP to 4-AP) recycling confines towards, used concentration of reactant was low, the reaction was monitor by UV-Vis spectrophotometer. For the first time we have performed the recycling study of AuNPs in the reduction of IBPEON to IBPE. In detail, as discussed above (**2.5**), we synthesized IBPE in first cycle. In second cycle in alcoholic liquor containing AuNPs was added IBPEON and $NaBH_4$ with constant stirring at room temperature. After completion of reaction, the product was isolated from ethyl acetate as organic layer and AuNPs remained in alcoholic layer. Finally the solvent from the product was removed by rotary evaporator. Repeated the similar procedure for next consecutive reaction cycles and recorded the percent yield of product in every cycles. We conclude that the AuNPs showed good catalytic activity against poisoning of catalyst after six consecutive reaction cycles.

RESULTS AND DISCUSSION

The AuNPs synthesised by chemical reduction method at room temperature in the presence of air and the colour changes from black to wine red with continue stirring shown in photographic image of AuNPs (Figure 1). The AuNPs was formed about four hours. The synthesised AuNPs was initially confirmed by UV. Vis Spectrometry. The surface plasmon resonance (SPR) band of AuNPs was at about λ 500 nm.

The morphological behaviour of nanostructured materials plays an important role in the catalytic activity. The synthesised AuNPs was characterized by TEM and HRTEM depicted in Figure 2. The bare AuNPs was formed pearl necklace [27] arrangement of

nanostructured material due to simply steady continuous stirring for 4 h (Figure 2). These necklaces of AuNPs were formed by simple chemical reduction method and without addition of stabilizers. The average diameter of necklace was found about 4 nm is very remarkable size resulted high surface area. In the inset of panel a, showed the Selected Area Electron Diffraction (SAED) pattern which confirmed the crystalline nature of particles. The crystalline nature of AuNPs was also confirmed by lattice fringes observed in HRTEM (Figure 2).

The catalytic activity of AuNPs was tested by well-known model reduction reaction of 4-nitrophenol (4-NP) to 4-aminophenol (4-AP) using $NaBH_4$ in the presence of AuNPs. The complete reduction of 4-NP to 4-AP took time of 13 minutes depicted in Figure 3. The isosbestic points confirmed that reduction of 4-NP and formation of 4-AP. Further, kinetics of the reaction was found pseudo-first order and rate constant was 0.167 ± 0.003 per minutes and it is proved the high catalytic activity and fast rate of reaction, this is due to the rigid, small necklace AuNPs was confirm by TEM and HRTEM images.

Table 1 Shows the percent practical yield in every catalytic cycle of AuNPs. The slight decrease in yield was observed. From this cycle count it was proved that the necklace shaped AuNPs showed excellent catalytic activity against poisoning of catalyst.

Spectroscopic characterization of IBPE

Lastly, the synthesized IBPE was characterized by using FTIR, and mass spectroscopy showed in Figure 4. The characterization data of IBPE as given below: 1-(4isobutyl)phenyl ethanol (IBPE) is isolated as viscous oil; b.p. 245-246 ^{0}C; FT-IR (KBr) cm^{-1}:

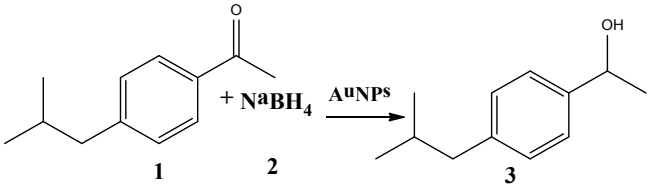

Scheme 1: Synthesis of IBPE from IBPEON in the presence of AuNPs

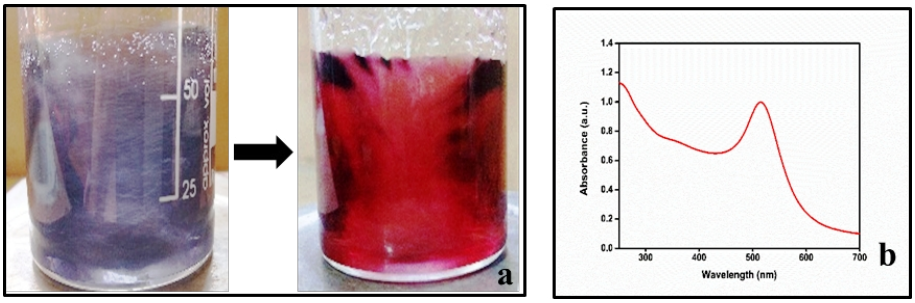

Figure 1: Panel a) synthesis of AuNPs and panel b) surface plasmon resonance (SPR) band of AuNPs

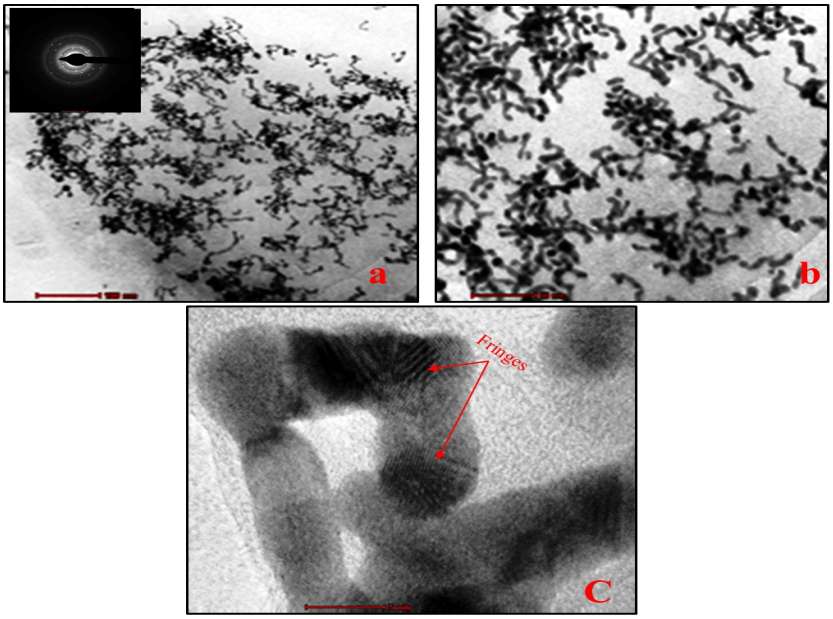

Figure 2: Panel a, b) TEM image of AuNPs and in inset panel a), is the selected area electron diffraction (SAED) pattern and panel c) HRTEM image of AuNPs

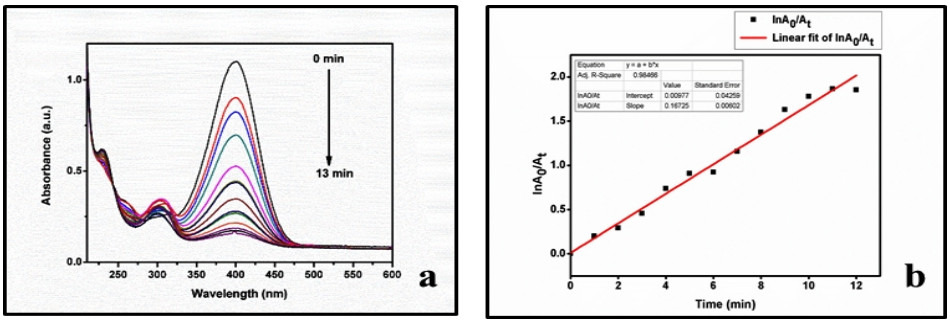

Figure 3: Panel a) Time dependent UV-Vis spectra for the catalytic reduction of 4-NP to 4-AP and panel b) Pseudo first order plot of AuNPs catalysed reduction of 4-NP to 4-AP by $NaBH_4$

Table 1: Percent practical yield of IBPE per cycle count

Cycle count	Percent yield of IBPE
1	92
2	89
3	86
4	85
5	81
6	77

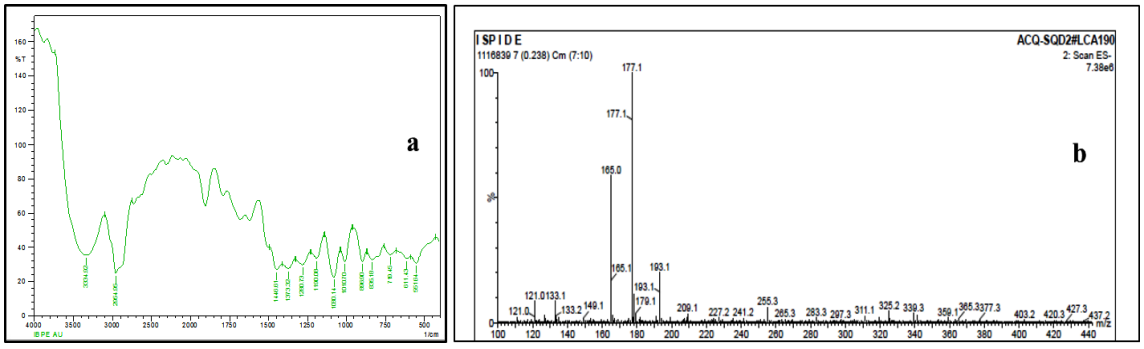

Figure 4: Panel a) FTIR spectra and panel b) mass spectra of IBPE

3334 (OH), 2954 (CH); ESI-MS: m/z = 177.1 $[M - H]^+$. The results were found to be well agreement with the reported literatures to conform the product IBPE.

CONCLUSION

In conclusion, From the TEM and HRTEM reveals necklace shaped gold nanostructured material materials (AuNPs) having excellent nano size thickness about 4 nm conforms large surface area and ultimately huge number of hydrogen was adsorbed on surface of AuNPs. This leads excellent catalytic activity of AuNPs against poison of catalyst. We efficiently evaluated the catalytic activity of AuNPs in the reduction of 4-NP to 4-AP by using $NaBH_4$. The recyclability study of AuNPs has been reported for the first time in the reduction of IBPEON – IBPE by using $NaBH_4$ in "Alcoholic AuNPs" and found very excellent yield of IBPE up to six consecutive reaction cycles. The reaction was completed within 15 minutes at room temperature. The results are first of its kind for using nanotechnology in the conversion of IBPEON to IBPE (Ibuprofen Intermediate) using aqueous Ethanol. The costly and important drug intermediate of Ibuprofen, IBPE was economically synthesized in the laboratory by environmentally benign process. In future, attempts will made to scale up the synthesis of 4-IBPE in pilot plant by collaboration with pharmaceutical industry. These results of the present investigation could be helpful for material chemistry scientists as well as organic researches to design the safer synthesis of important commonly used pharmaceutical drugs.

Acknowledgements

The authors would like to thank BSR-UGC, New Delhi for financial support. In addition SAIF, Chandigarh, Punjab University for Spectroscopy characterizations, SAIF, IIT Bombay for TEM characterization.

REFERENCES

[1] D. Astruc, *Nanoparticles and Catalysis*. Vol. 1, Weinheim: Wiley-VCH, **2008**.

[2] G. Frens, *Nature,* **1973**; 20-22.
[3] D. V. Leff, P. C. Ohara, J. R. Heath and W. M. Gelbart, *J. Phys. Chem*., **1995**, 7036-7041.
[4] K. Mallick, Z. L. Wang, and T. Pa, *J. Photochem. Photobio. A: Chem*., **2001**, 75-80.
[5] T. K. Sau, A. Pal, N. R. Jana, Z. L. Wang, and T. Pal, *J. Nano. Res*., **2001**, 257-261.
[6] K. Okitsu, Y. Mizukoshi, T. A. Yamamoto, Y. Maeda, and Y. Nagata, *Mat. Lett.,* **2007**, 3429-3431.
[7] C. Li, W. Cai, C. Kan, G. Fu, and L. Zhang, *Mat. Lett*., **2004**, 196-199.
[8] M. J. Firdhouse, P. Lalitha and S. K. Sripathi, *Digest. J. Nanomat*. *Biostr*., **2014**, 385-393.
[9] J. Y. Song, Hyeon-Kyeong Jang and B. S. Kim, *Pro. Biochem*., **2009**, 1133-1138.
[10] B. Nikoobakht and M. A. El-Sayed; *Langmuir*, **2001**, 6368-6374.
[11] T. K. Sau, and C. J. Murphy; *Langmuir,* **2004**, 6414-6420.
[12] L. Wang, W. Mao, D. Ni, J. Di, Y. Wu, and Y. Tu, *Electrochem. Comm*, **2008**, 673-676,
[13] N. N. Long, C. D. Kiem, S. C. Doanh, C. T. Nguyet, P. T. Hang, N. D. Thien, and L. M. Quynh, *In. J. Phys*., *Conference Series*, **2009**, 012026, IOP Publishing.
[14] A. Molnar, A. Sarkany, and M. Varga, *J. Mol. Cat. A:* Chem., **2001**, 185-221.
[15] A. Borodzinski; *Catal. Let.,* **2001**, 169-175.
[16] Y. Li, E. Boone and M. A. El-Sayed, *Langmuir,* **2002**, 4921-4925.
[17] J. Le Bars, U. Specht, J. S. Bradley, and D. G. Blackmond, *Langmuir*, **1999**, 7621-7625.
[18] M. Arenz, K. J. Mayrhofer, V. Stamenkovic, B. B. Blizanac, T. Tomoyuki, P. N. Ross, and N. M. Markovic, *J. Am. Chem. Soc*., **2005**, 6819-6829.
[19] A. A. Herzing, C. J. Kiely, A. F. Carley, P. Landon and G. J. Hutchings, *Science*, **2008**, 1331-1335.
[20] G. A. Martin, *J. Cat*., **1979**, 452-459.
[21] E. G. Derouane, *Cattech*, **2001**, 214-225.
[22] M. Poliakoff, and P. Licence, *Nature,* **2007**, 810-812.
[23] S. Saha, A. Pal, S. Kundu, S. Basu, and T. Pal, *Langmuir*, **2009**, 2885-2893.
[24] S. Panigrahi, S. Basu, S. Praharaj, S. Pande, S. Jana, A. Pal, S. K. Ghosh, and T, Pal, *J. of Phy. Chem. C;* 4596-4605.
[25] T. Aditya, A. Pal, T. Pal, *Chem. Commun.,* **2015**, 9410-9431.
[26] L. Ai, H. Yue, J. Jiang, J. Mater. Chem., **2012**, 23447-23453.
[27] M. S. Bakshi, G. Kaur, F. Possmayer, and N. O. Petersen, *J. Phys. Chem. C*., **2008**, 4948-4953.

Use of High Pressure Autoclave for Chemical Recycling of Plastic Wastes

Vishvanath Zope

Head, Department of Chemistry, Moolji Jaitha College, Jalgaon, Maharashtra, India

Abstract *— High pressure autoclave of 500 mL capacity, facilitated with temperature control panel working under maximum pressure up to 100 kg/ cm^2 or 1500 psi, and maximum temperature up to 250^{O}C was found to shorter the reaction time for chemical recycling of plastics wastes. Depolymerisation of polyester waste was carried out by saponification reaction. Yield of depolymerised product was obtained up to 85% for 2.5 h reaction time. Product obtained was characterized by chemical as well as instrumental analysis such as M.P. (sublimation), acid value and FTIR Spectra. The results agree with pure Terephthalic acid (TPA). Chemical kinetics of this reaction shows that it is a first order reaction with respect to polyethyleneterephathalate (PET) concentration which is in the order of 10^{-2} min^{-1}.*

Keywords — *Depolymerization, Kinetics, Thermodynamics, Terephthalic acid*

I. INTRODUCTION

Polyethylene terephthalate (PET) is semi-crystalline thermoplastic polyester widely used in the form of fibers, sheets and films. PET is characterized by high mechanical strength and low permeability to gases, with good aesthetic appearance. It is non-toxic material having high resistance to atmospheric and biological agents.

PET is condensation thermoplastic polymer produce by the reaction of terephthalic acid (TPA) with mono ethylene glycol. PET was first used commercially in the 1950s as Terylene and Dacron in the form of fiber. Now a day PET is commonly and widely used in the form of film for X-ray photographs, magnetic recording tapes, packaging and many industrial uses. In the 1970s technology was developed to use PET as rigid container. Since then the container market has grown very rapidly. Particularly the mineral bottles, soft drink bottles made by PET are accepted by the society. Polyester is the major fiber used in non-woven interlinings, interfacing, filtration media, surgical and medical products, agricultural clothes, coated and laminated packaging.

Since the first recycling of PET in 1977 (Miller 2002), many studies have been conducted to investigate PET recycling methods (Helwani et al. 2009; Patterson 2007; Yoshioko et al. 1994, 2001), and the recovery rate of consumed PET has been consistently increasing. The world consumption of PET packaging is expected to about 19.1 million tons by 2017, with 5.2% increase per year between 2012 and 2017 (Smithers Pira 2012). The recycling of plastic wastes is well illustrated[1] by Figure 1.

Figure 1 Recycling loop.

On the basis of chemical composition, manufacturing and conversion process and recycling techniques, PET is treated as one of the best eco-friendly polymer in world. PET bottles are extensively consumed for drinks and beverages in residential houses, restaurants, stadium, railway stations airports, entertainment venues and other public places, therefore collection and recycling of post-consumer PET bottles need not be overlooked. Disposal of plastic waste into landfills has become increasingly prohibited due to high cost, legislative pressure and environmental pollution. Growing environmental awareness and reduction in landfill have promoted plastic recycling program in most of the countries[2-3]. Currently, however only 25 % of plastic waste is being recycled. The PET generally has second highest scrap value after aluminum[3]. Hydrolysis of PET can be done by high pressure and temperature to depolymerise PET into TPA and EG. Many researchers reported that hydrolysis of PET with water can be either acid catalyzed or base catalyzed[4-5]. In our study besides these methods we are successful to depolymerise PET at high temperatures and pressures without catalyst[6]. In our study these processes are under taken for investigations of velocity constants, frequency factor, enthalpy of activation[7-8], entropy of activation, free energy of activation, and equilibrium constant. These data are required by chemical engineers for designing of reactor or to scale up the established equipment.

II. EXPERIMENTAL

A. *High Pressure Autoclave*

It was provided with vent valve, liquid sampling valve, gas inlet valve, automatic cooling system, temperature alarm system etc. Liquid sample after definite time interval can be withdrawn from liquid sample valve. The autoclave was equipped with silver rupture disc having a burst rating of 1600 psi pressure at 250^{O}C. In order to mix the reaction mixture homogeneously autoclave was facilitated with stirrer having magnetic drive. The magnetic drive was of zero leakage and maintenance free, which was facilitated with magnetic coupling directly driven by the motor. High energy permanent magnet was fixed inside the inner rotor and on inner side of the external shell.

Fig.2 High Pressure autoclave

The gland (magnetic drive) was always kept cooled by supplying ordinary tap water through gland cooling system to increase lifetime of the system. The cooling was continued even after the heating was stopped otherwise the temperature of the magnet may increase due to heat transfer. Magnets can withstands maximum up to only 70^{O}C. Thereafter at about 80^{O}C they lose their property. This will render the drive useless as its torque will reduced to 20%. For 0.5 L autoclave, the torque capacity of magnetic drive is 20 kg.cm. in maximum permissible viscosity of the liquids up to 50,000 centistokes.

Always the precautions were taken that cylinder gas pressure should more than the autoclave pressure to avoid flow of autoclave reaction mixture in to cylinder, as it may create serious problem. First the gas inlet valve was closed and gas pipeline was pressurizing by releasing the gas from the cylinder. As soon as the pressure gauze reading of hose pipe line was more than the inside pressure of autoclave, gas inlet valve was opened and charged the gas to achieve desired pressure and inlet valve was closed tightly. To release the gas at the end of the reaction, vent valve was used. The sample for the analysis was withdrawn at definite time intervals from liquid sample valve.

B. *Depolymerization of PET waste at high temperature and high pressure:*

The PET waste was chilled for its brittleness and grounded in to desired particle size of 425µm to create maximum surface area for heat and mass transfer in the reaction vessel. 0.5 L capacity high pressure auto autoclave was used for all hydrolytic depolymerisation experiments. The autoclave was well equipped with constant rotating stirrer at the speed of 500 rpm, which ensures the proper mixing of reaction mixture.

10 g of PET waste and 300 mL water of very high purity of HPLC grade (1:30 w/v), were charged in vessel of autoclave. The vessel was heated for 2 hours. After the specified time interval and the reaction temperature, the vessel was cooled suddenly and removed from heating collar. The vessel was subsequently opened and the product was removed. It was treated with sodium hydroxide to form sodium salt of terephthalic acid then acidified with hydrochloric acid; a white pure precipitate of TPA was obtained. It was filtered, dried and weighed. Sodium hydroxide treatment followed by hydrochloric acid was given in order to obtain pure TPA. After drying it was grounded up to fine powder using mortar and pestle.

Similar experimental procedure was repeated for various pressures such as 100, 200, 300, 400, 500, 600, 700, and 800 psi. at 100, 150, 200 and 250^{0}C respectively. Similarly for kinetic and thermodynamic studies, the experiments were carried out for the reaction time 30, 60, 90, 120 and 150 min. at 200 and 250^{0}C maximum temperatures. All these experimental processes were carried out in batches.

III. RESULT AND DISCUSSION

A. ***Kinetics of hydrolytic depolymerisation of PET waste*** The kinetic study of depolymerisation was under taken on the basis of product depolymerised and its residue. The velocity constant of depolymerisation was calculated by using formula,
$k = [2.303/t] \log [a/(a-x)]$,
Where, a = initial weight of PET waste in gram,
k = velocity constant of the reaction,
x = amount of PET depolymerised in gram at time‘t’.
On the basis of results obtained, the velocity constants 1.773×10^{-2} min^{-1} and 6.909 min^{-1} were recorded for the depolymerization reaction at 200 and 250^{0}C

B. ***Verification of First Order Kinetics*** The straight line natures of the graph of log {a / (a-x)} versus time in minute and almost passing through origin shows the first order reaction kinetics. Slope gives the values of velocity constants 1.773×10^{-2} and

6.909 x10^{-2} min^{-1} at 200 and 250 ^{O}C respectively Fig.3.

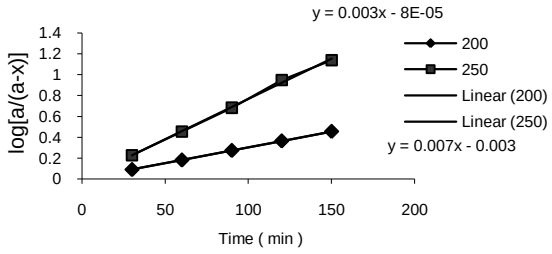

Fig. 3- Verification of First Order Kinetics of Depolymerisation of PET Waste at 200 and 250^{O}C Temperatures.

.

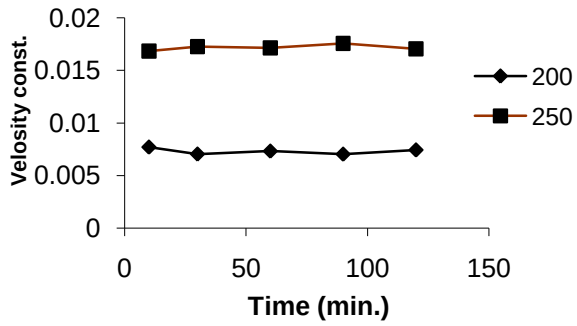

Fig.4 Graph of velocity constants versus time

Parallel nature of the Fig. 4 shows that the velocity constants remain constant at both the temperatures. At higher temperature i.e. 250^{O}C it is about four times higher than at 200^{O}C.

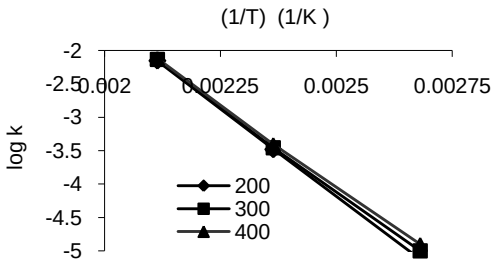

Fig. 5: Variation of log K With 1/ T At 200, 300 And 400 psi Pressure

C Energy of Activation

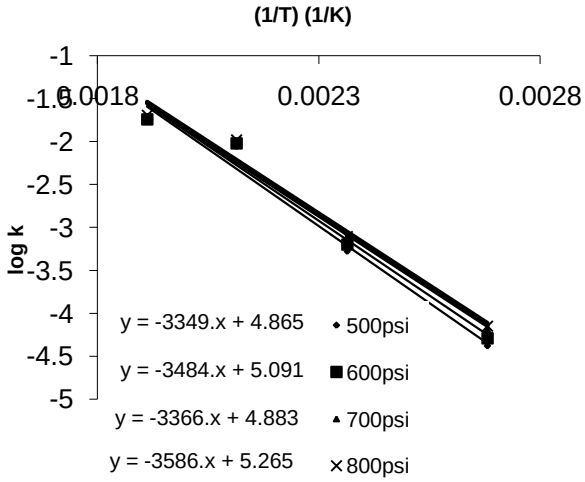

Fig. 6 Variation of log K With 1/ T At 500, 600 700 And 800 psi Pressure

The energy of activation and frequency factor are obtained by plotting Arrhenius graph log k versus 1/T at various pressures as shown in Figs.5 and 6**.** The intercept and slop of the Arrhenius plot give frequency factor and energy of activation respectively. These two thermodynamic parameters at various pressures are shown in Table 1**.** It is clear from above results that there is no significant increase in values of energy of activation and frequency factor with varying the pressure from 500 to 800 psi.

Table 1 shows the values of intercepts and slops at various pressures 200, 300, 400, 500, 600, 700, and 800 psi. These values provide frequency factors and energy of activations. The enthalpy of activation was calculated by using values of energy of activations at 200^{O}c.

Table.1 Thermodynamic parameters

Pressure psi.	**Slope**	**Ea $KJmole^{-1}$**	**ΔH $KJmole^{-1}$**	**Intercept**	**Frequency factor (A) x10^{5} min^{-1}**
200	-4900	9135	9127	8.21	807.6
300	-5041	8796	8788	8.49	315.5
400	-5235	8551	8543	8.90	165.1
500	-3349	6257	6249	4.86	1.841
600	-3484	6079	6071	5.09	1.233
700	-3366	5874	5866	4.88	0.765
800	-3586	5844	5836	5.26	0.734

IV. CONCLUSIONS

1. High pressure autoclave was found to be the effective reactor to shorten the reaction time.
2. Neutral water hydrolysis of PET is only possible using High pressure autoclave above 200 psi pressure.
3. Neutral water hydrolysis (depolymerization) of PET was found to be first order kinetics having velocity constant value in the order of 10^{-2} min^{-1}.
4. Energy and enthalpy of activations decreases with increase in pressure indicating less amount of energy is required for reaction.

ACKNOWLEDGMENT

Author is very thankful to Prof. S. Mishra, Institute of Chemical Technology, N. M. U. Jalgaon, Maharashtra for his continuous motivation and inspiration regarding quality research.

REFERENCES

[1] Sang Ho Park and Seong Hun Kim, *Poly (ethylene terephthalate) recycling for high value added textiles*1:1 Park and Kim Fashion and Textiles 2014.

[2] Macck, H.; *Plastic Recycling*, Popular plastic and Packaging, 41,1992.

[3] Polymer Recycling, *Wiley Series in Polymer Science*, 1997.

[4] Paszun, D.; Spychaj, T.; *Recycling of Poly(Ethylene terephthalate) to obtain solid Cross-linked Agents, Proceedings of the National Conference on Polymer Environment Recycling*, Szczecin-Miedzyzdroje (in Polish), 221, 1995.

[5] Ostrysz, R.; Penczek, P.; Sniezko, A.; *Use of Waste from the Production of PET for Production of polyester and alkyd Resins, Khim. Ind*. **2**, 1995.

[6] Yoshioka, T.; Okayama, N.; Okuwaki**,** A.; *Kinetics of Hydrolysis of PET Powder in Nitric Acid a Modified Shrinking Core- Model*; *Ind. Eng. Chem. Res.*; **37**, 336, 1998.

[7] Yashioka, T.; Motoki.; Okuwaki, *A.; Kinetics of Hydrolysis of Poly(Ethylene Terephthalate) powder in Sulfuric Acid by a Modified Shrinking –Core Model*; *Ind. Eng. Chem. Res.*; **40**, 75, 2001.

[8] Mishra, S; Zope, V.S.; and Goje, A.S.; *Kinetics and Thermodynamics of Hydrolytic depolymerization of Poly (Ethylene Terephthalate) at High Pressure and temperature, J. Appl. Polym. Sci.* **90** (12), 3305,2003

Fe_3O_4-polyaniline nanofibers synthesis in non-ionic surfactant based swollen liquid crystals

Shivkumar Y. Patil[1], Pramod P. Mahulikar[1], Sandeep J. Pawar[1], Vishwanath. S. Zope[2*]

1 School of Chemical Sciences, North Maharashtra University, Jalgaon, 425001 Maharashtra, India.

2 Department of Chemistry, Moolji Jaitha College, Jalgaon 425001 Maharashtra, India

Graphical abstract

Abstract

Polyaniline (PANI) and Fe_3O_4-PANI composite nanofibers were synthesized for the first time using non-ionic surfactant based "soft templates". Prepared lamellar mesophase with PANI and nanocomposites was confined by using polarized optical microscope. The synthesized nanocomposite showed PANI fibre diameters ranging from 70-300 nm as observed in FESEM. For the electrochemical measurements PANI and Fe_3O_4-PANI nanocomposite material was coated on stainless steel plates and 1M H_2SO_4 was used as a electrolyte. The capacitance measured by CV showed pseudocapacitance behaviour of PANI and Fe_3O_4-PANI and the nano Fe_3O_4-PANI modified electrodes showed higher value of the capacitance as compared to PANI nanofibres.

Keywords: Swollen liquid crystal; magnetic nanoparticles; polyaniline nanofibers; supercapacitors.

Corresponding author:

To whom correspondence should be addressed:

Prof. Dr. V. S Zope

Department of Chemistry,

Moolji Jetha College,

Jalgaon 425 001 Maharashtra,

India

Mobile No: +91 9422224616

1. Introduction

Synthesis of nanomaterials with the controlled morphology of nanostructures is new advancement in the field of nanoscience and nanotechnology [1]. Surfactant based swollen liquid crystals (SLCs) such as hexagonal and lamellar mesophases are structure directing templates in new synthetic way for material chemistry [2]. The "hard" template constitute solid like mesoporous silica which uses harsh chemical treatments after post synthesis. On the other hand, use of "soft" templates is easy as well as convenient for separation of motifs like polymers and surfactants [3]. Polyaniline (PANI) is one of the most important conducting polymer (CP) because of high conductivity, ease to synthesis, low cost and good environmental stability [4]. Potential application of PANI derivatives were reported in the field of batteries, capacitors, fuel cells and gas sensing devices [5-7]. It can be synthesized via chemical, electrochemical and template assisted methods [8]. Nanocomposites of CPs with inorganic materials such as metal oxides, carbon based nanostructures have been thoroughly utilized in various applications such as electrochemical sensors, energy storage and catalysis [9-10]. Synthesis of Fe_3O_4 nanoparticles are emerged as mechanical, electromagnetic shielding materials and catalyst for degradation of environmental pollutants [11].

Additionally, Fe_3O_4 nanoparticles based nanocomposites are synthesized by using variety of methods such as chemical, blending with co-precipitation, picker emulsion and interfacial polymerization to produce core-shell nanostructures [12-13]. Literature reported hitherto revealed that the nanocomposites of Fe_3O_4 with PANI were used for chemical oxidation polymerization for microwave absorbents and electromagnetic shielding coatings [12, 14].

Recently, synthesis of organic conducting polymers and metal nanoparticles in hexagonal swollen liquid crystals (SLCs) has been successfully used for the chemical polymerization of 1-D PEDOT, PANI and core shell structures of Au-PANI [3, 15-16]. SLCs

are formed by using quaternary system of oil, water, surfactant and co-surfactant and they can be used as hexagonal SLCs as soft templates for synthesis of Pt and Pd nanostructures [17-18].

In the present study, we have reported the first time nanoscale synthesis of 1-D PANI and Fe_3O_4-PANI nanostructures. We have designed nanofibers of these two motifs in swollen lamellar mesophase based on non-ionic surfactant Triton X-100. *In-situ* chemical oxidation polymerization of PANI and Fe_3O_4-PANI nanocomposite in swollen lamellar mesophase was performed using ammonium persulfate (APS) as an oxidant.

2. Experimental

2.1 *Materials*

The non-ionic surfactant (Triton X-100) was procured from fisher-scientific and aniline (99.5%), ammonium persulfate (98%), cyclohexane (99.8%) and 1-pentanol (98%) were purchased from Merck.

2.2 *Synthesis of Polyaniline (PANI) in lamellar mesophase*

2.4 g of non-ionic surfactant Triton X-100 was dissolved in 2 mL of 0.1 M HCl solution at 35 ^{o}C. After complete dissolution of the surfactant, 3.3 mL of cyclohexane (oil) containing 4 mM of aniline monomer was added to the surfcatant mixture with vigorous vortexing. 1-Pentanol (co-surfactant) was then added to the mixture and strongly vortexed for a few minutes [19]. This resulted into perfectly transparent and unstable gel that is a lamellar mesophase. Then 8 mM of APS initiator was added to this mixture with continuous vortexing, to afford a dark green colored of PANI fiber in mesophase. **(Scheme 1)**

2.3 *Synthesis of Fe_3O_4-PANI in lamellar mesophase*

Synthesis of Fe_3O_4 nanoparticles was achieved according to reported method [20]. Aqueous 0.1 M HCl (2 ml) with magnetic nanoparticles was sonicated and 2.4 g of non-ionic surfactant was added in it. After complete dissolution of the surfactant, 3.3 mL of cyclohexane (oil) containing 4 mM of aniline monomer was added to the mixture with vigorous vortexing (monomer:Fe_3O_4, 4:1). Consequently 1-pentanol (co-surfactant) was added to this mixture and strongly vortexed for a few minutes. This leads to a perfectly unstable gel: a lamellar mesophase. Then APS as initiator was added this phase with continuous vortex resulting into subsequent color change. (Fig. S1 supporting information)

The lamellar mesophase was optimized by the ratio of aniline: APS (2:1) for synthesis of PANI nanofibers and its nanocomposites in soft templates. In order to characterize the synthesized material in lamellar mesophase, the mesophase was destabilized by iso-propanol and double distilled water centrifugation cycle. The dried samples were analyzed by FTIR, FESEM, XRD, TGA, UV-Visible spectrophotometer and electrochemical measurements.

Scheme 1. Schematic representation of PANI and nanocomposites synthesized in non-ionic surfactant assisted soft templates.

2.4 *Charecterization*

Swollen liquid crystals (SLCs) (before and after polymerization) were characterized by polarized optical microscope (Leica DM 750 P). FESEM observations were performed with S-4800 Hitachi, USA at an accelerating voltage of 30 kV. FTIR spectra of PANI nanofibers were analyzed by Alpha instrument from Bruker in the range 400 to 4000 cm^{-1}. XRD patterns of the samples were conducted with D8 Advance Bruker Ltd. Germany Diffractometer using Cu Kα radiation. TGA was recorded using Perkin Elmer 4000 TG Analyzer. UV-Visible spectra were recorded by Agilent Technologies Carry 60 UV-Vis spectrophotometer.

2.5 *Electrochemical Measurements*

Cyclic voltammetry measurements were performed with an Autolab PGSTAT-30 electrochemical workstation (Metrohm, India), using three-electrode system. For modifications of SS plates, 85 % of synthesized nanocomposite Fe_3O_4-PANI and PANI, 5 % PVDF and 10 % carbon black were dissolved in N-methyl pyrrolidone (NMP) solvent. The modified electrodes were prepared by dip coating of prepared nanocomposites solution on polished stainless steel plates [21]. For the electrochemical measurements modified SS electrodes were used as a working, platinum wire as counter and Ag/AgCl as a reference electrodes. The CV curves were collected at different scan rates ranging from 10 to 100 mV/s with the potential range of -0.2 to 1 V. The electrochemical tests were carried out in 1 M H_2SO_4 electrolyte solution at ambient temperature.

3. Results and Discussion

Fig. 1. Polarized optical microscope images of (a) lamellar mesophase, (b) synthesized PANI in mesophase and (c) synthesized Fe_3O_4-PANI in mesophase using Triton X-100.

Polarized optical microscope image of lamellar mesophase was found to be clear as shown in Fig. 1a. Small dark blue colored particles were observed in Fig. 1b that depicted the successful synthesis of PANI in mesophase. Similarly, Fig. 1c showed the Fe_3O_4 doped nanocomposites in mesophase. As reported by Ghosh et.al. [16] Synthesized PANI and

Fe_3O_4-PANI nanocomposites in mesophase for dark blue colored particles are entrapped into the lamellar mesophases are believable and are more reliable.

Fig. 2. FESEM images of (a) Fe_3O_4, (b, c) PANI and (d, e) Fe_3O_4-PANI.

The FESEM study demonstrated spherical form of Fe_3O_4 nanoparticles with an average diameter of 40 nm as shown in Fig. 2 a. Synthesized PANI using Triton X-100 assisted template showed longer, uniform and smooth surfaces of the PANI nanofibres with an average diameter of 200-300 nm (Fig. 2b and c). Fe_3O_4 nanoparticles doped on the surfaces of PANI showed Fe_3O_4 nanoparticles decorated nanofibers with an average diameter of 100-130 nm. (Fig. 2d & 2e)

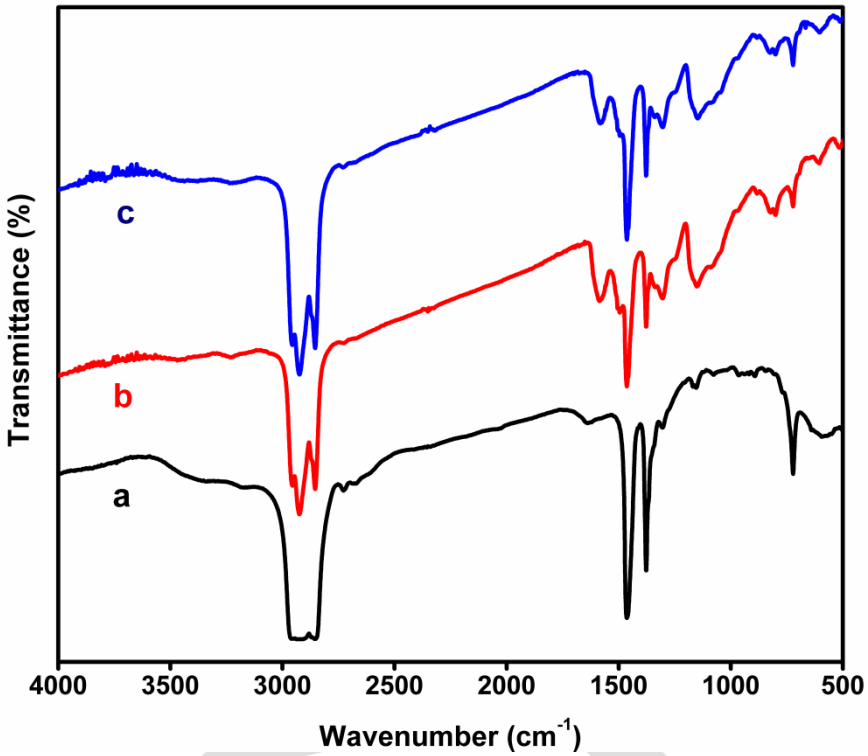

Fig. 3.FTIR spectra of (a) Fe_3O_4, (b) PANI and (c) Fe_3O_4-PANI.

The FTIR spectra of Fe_3O_4, PANI and PANI-Fe_3O_4 composite are shown in Fig. 3. In the IR spectrum Fe_3O_4 (Fig. 3a), the peak at 577 cm^{-1} was attributed to the characteristic band of Fe-O vibration. The IR spectrum of PANI (Fig. 3b), the band at 1301 cm^{-1} was corresponds to the stretching vibration of C-N, 1147, and 821 cm^{-1} were corresponded to out of plane deformation of C-H in the 1,4-disubstituted benzene ring. In IR spectrum of Fe_3O_4-PANI nanocomposites (Fig. 3c) the characteristic band at 1582 cm^{-1} was due to the C=C stretching deformation of quinoid and benzenoid ring of PANI. The IR spectra confirmed that the Fe_3O_4 nanoparticles were decorated on the surface of PANI nanofibres.

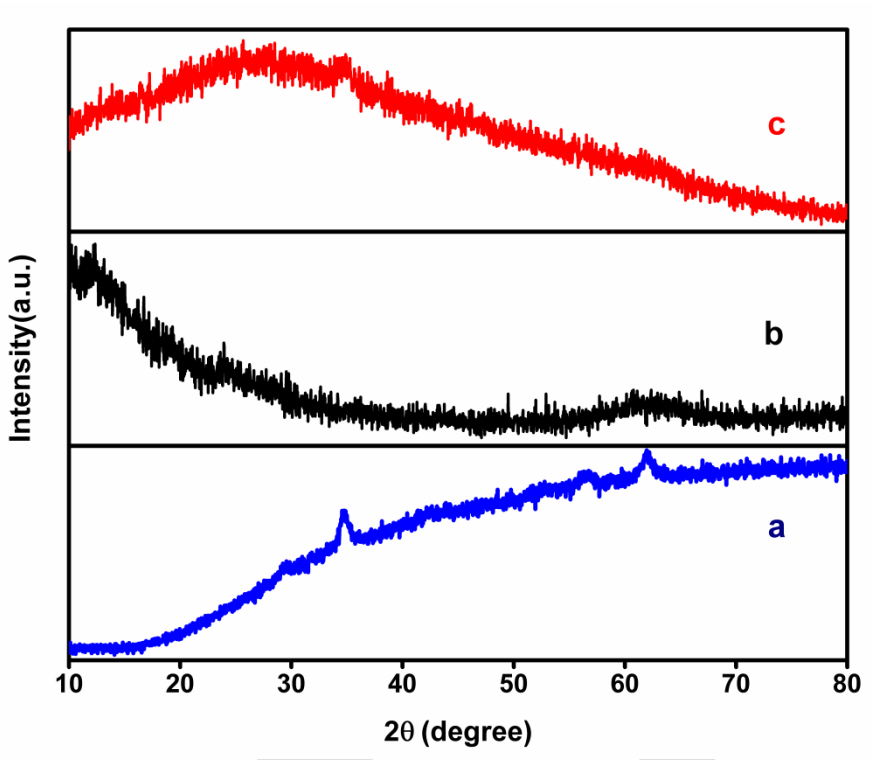

Fig. 4. XRD of (a) Fe_3O_4, (b) PANI and (c) Fe_3O_4-PANI.

A comparative x-ray diffraction pattern of pristine Fe_3O_4, PANI and Fe_3O_4-PANI nanocomposite are depicted in Fig. 4. In case of Fe_3O_4 nanoparticles, Bragg's peaks at 29.37, 34.78, 42.32, 52.85, 56.52 and 62.15 are ascribed to (220), (311), (400), (422), (511) and (440) planes respectively, which shows that the Fe_3O_4 nanoparticles are with cubic spinel structure. For PANI (Fig. 4b) 2θ = 19.47 and 24.04 were due to the periodicity that is parallel and perpendicular to the molecular chains of PANI and its polycrystalline in nature. For composites material (Fig. 4c), a broad hump like shape was observed however, Bragg's peak at 34.78^o confirmed the successful grafting of Fe_3O_4 nanoparticles on the surface of PANI nanofibres.

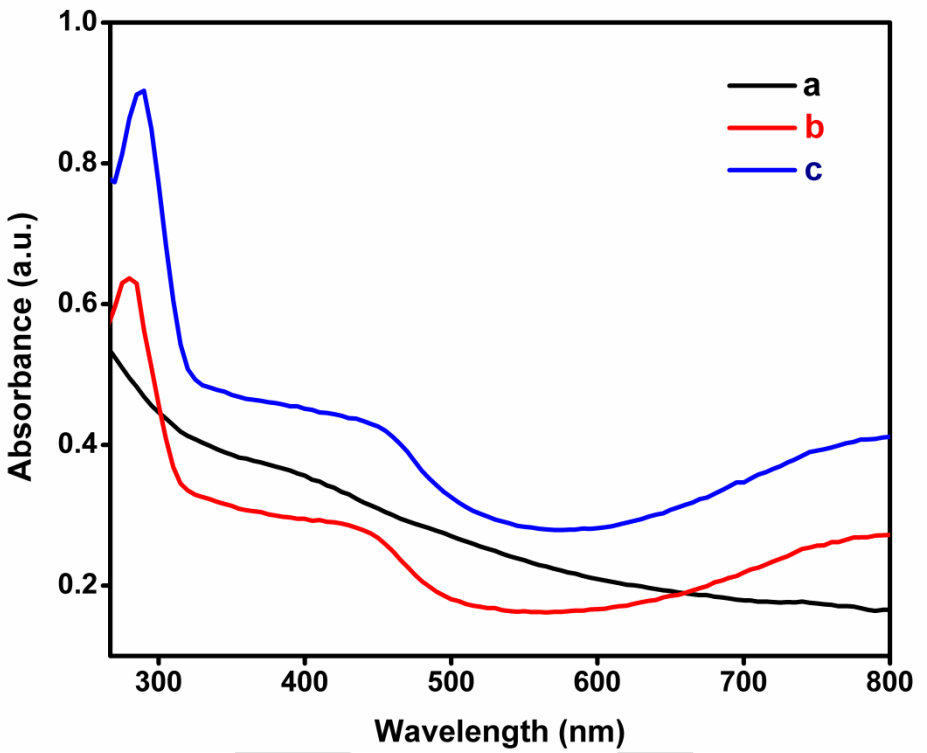

Fig. 5. UV-Visible spectra of (a) Fe_3O_4, (b) PANI and (c) Fe_3O_4-PANI.

No significant absorption peaks were observed for in Fe_3O_4 nanoparticles (Fig. 5a). PANI-Fe_3O_4 exhibited two characteristic bands at 280 and 443 nm, which could be attributed to the π-π* transition of the benzenoid ring and the benzenoid-quinoid excitonic transition, respectively (Fig. 5c).

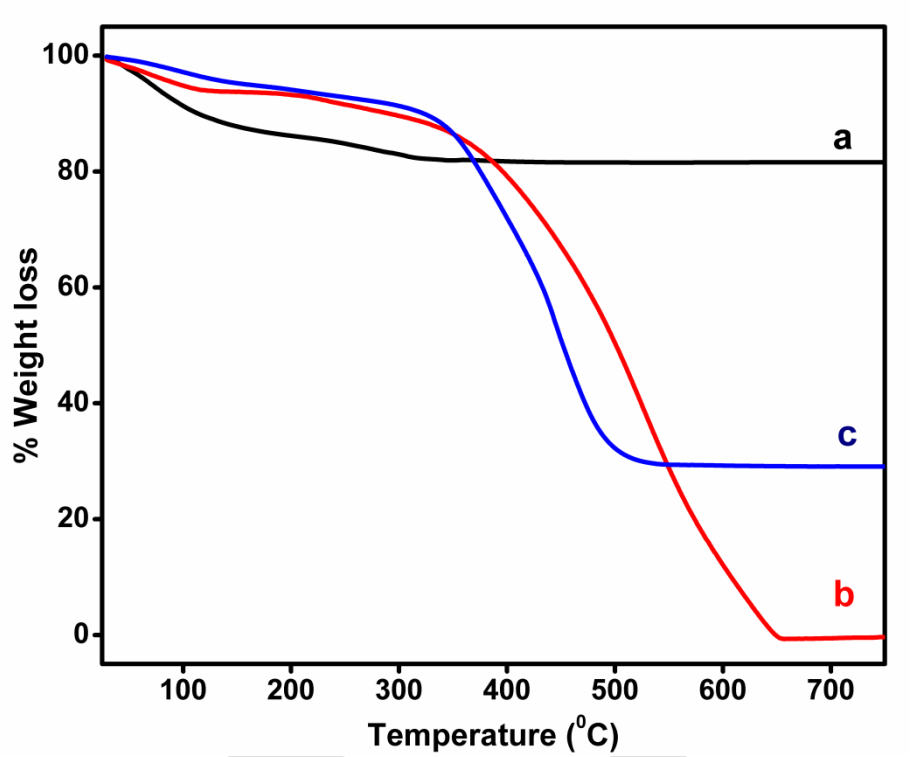

Fig. 6. TGA spectra of (a) Fe_3O_4, (b) PANI and (c) Fe_3O_4-PANI.

In thermal analysis, Fe_3O_4 nanoparticles showed weight loss above 200 ^{0}C was because of the oxidation of Fe_3O_4 to γ-Fe_3O_4 and further weight loss of 19% in the range of 300 to 750 ^{0}C (Fig. 6a). In PANI samples two stage degradation was observed, first stage at 130 ^{0}C due to water or moistures and second stage complete degradation of backbone of polymer chain (Fig. 6b). Lastly, Fe_3O_4 doped composites first weight loss similar water molecules eliminate and second step 130 to 750 ^{0}C weight loss is 30 % due to the incorporate Fe_3O_4 nanoparticles (Inorganic residue) on the surface of polymeric nanofibers (Fig. 6c). This is confined that the thermal stability of nanocomposites is enhanced than the PANI nanofibers.

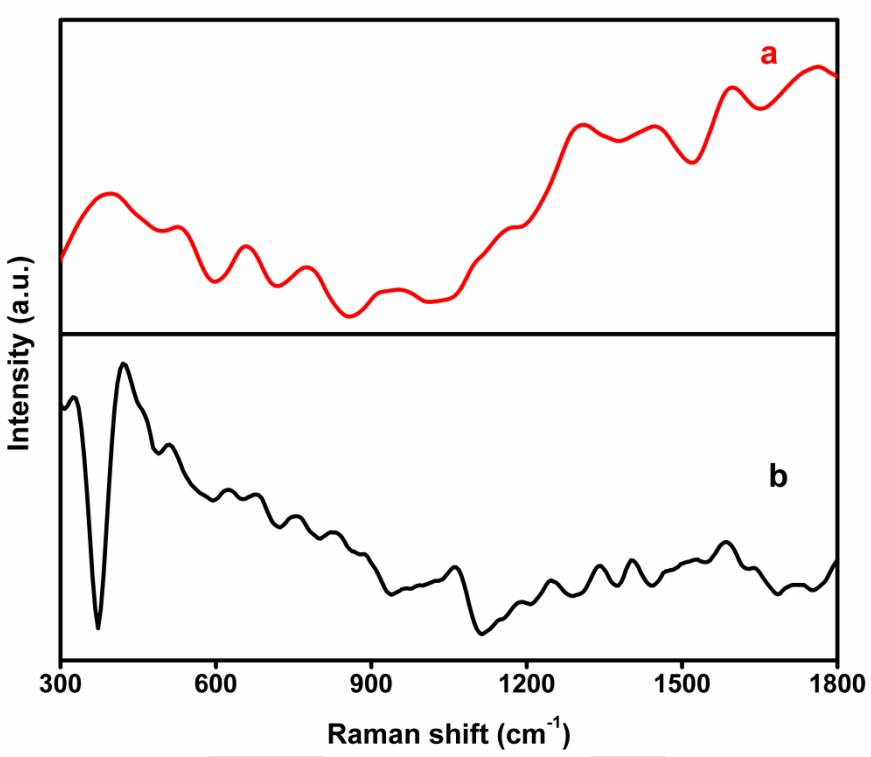

Fig.7. Raman spectra of (a) Fe_3O_4 and (b) Fe_3O_4-PANI.

In Raman spectrum of Fe_3O_4 nanoparticles (Fig. 7a), the peaks at 660 and 536 cm^{-1} were ascribed to the A1g and T2g modes of Fe_3O_4 nanoparticles. However in the spectrum of Fe_3O_4-PANI nanocomposites (Fig. 7b), the additional peaks at 1176, 1336, 1467 and 1584 cm^{-1} were corresponded to the C-H bending of quinoid/benzenoid ring, C-N stretching, C=N stretching of quinoid ring and C-N stretching of benzenoid ring respectively, that confirmed the grafting.

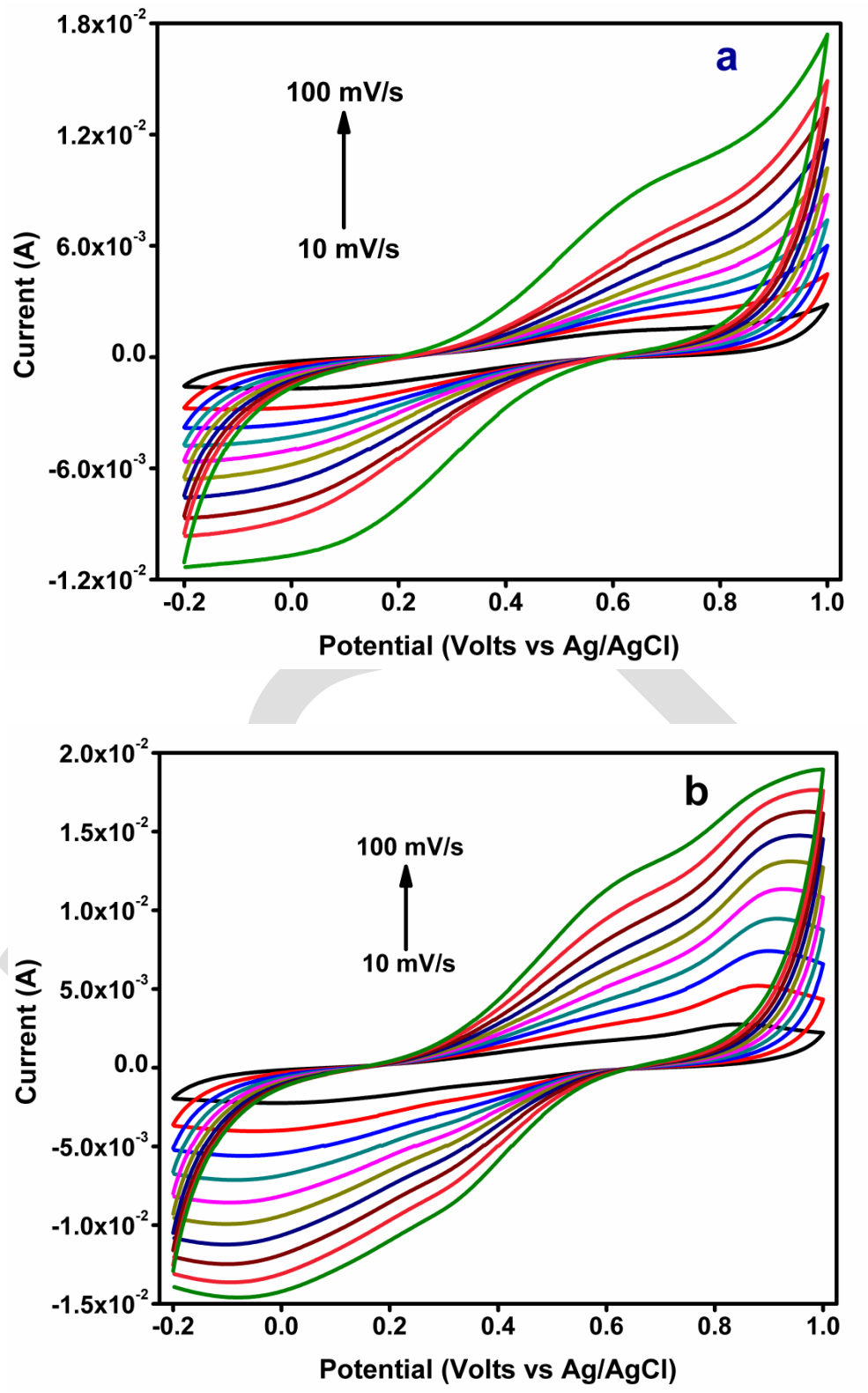

Fig. 8. Cyclic voltammetry of (a) PANI and (b) Fe_3O_4-PANI nanocomposites at 10 to 100 mV/s scan rates the potential range -0.2 to 1 V in 1M H_2SO_4.

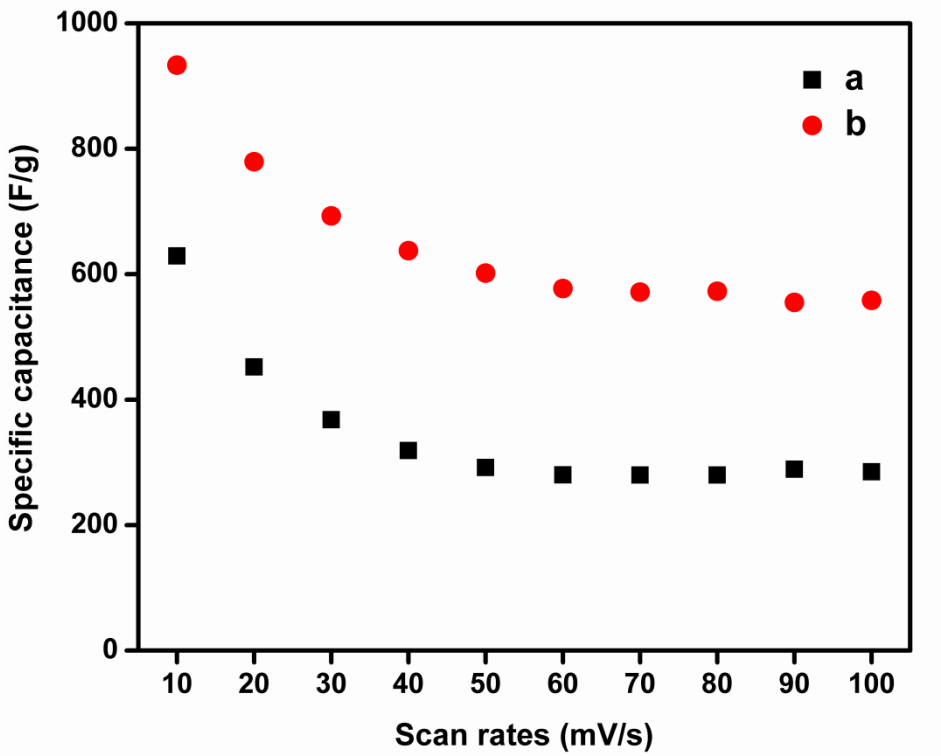

Fig. 9. Specific capacitance of (a) PANI and (b) Fe_3O_4-PANI nanofibers from CV vs. scan rates.

Cyclic voltammetry (CV) was used to explore electrochemical properties of PANI and Fe_3O_4-PANI at 10, 20, 30, 40, 50, 60, 70, 80, 90, 100 mV/s scan rates in 1M H_2SO_4 aqueous solution with the potential range of -0.2 to 1 V vs. Ag/AgCl. The CV curves of PANI nanofibers depicted two pairs of redox peaks (Fig. 8a), which is due to the pseudocapacitance behaviour. The first pair of redox peak was located at low potential corresponded to the redox transition of PANI from leucoemeraldine to emeraldine state and the redox peak located at high potential was attributed to the transformation from emeraldine to pernigraniline state [22]. The Fe_3O_4-PANI nanocomposite showed increasing CV loops compared to PANI its good sign for the capacitance (Fig. 8b). The increasing scan rates with increasing current clearly indicated that the composites material and PANI nanofibers electrodes have good rate stability [23].

Specific capacitance of the electrode materials was calculated by using following equation from CV curves,

$$C = \int Idv/2mvV$$

Where, C is specific capacitance of the mass of electroactive materials (F/g), I is the response current (A), V is potential (V), v is potential scan rate (V/s) and m is the mass of active electrode materials (g). Specific capacitance for PANI was found to be 629.16 and that of Fe_3O_4-PANI was 933.33 F/g at 10 mV/s scan rate (Fig. 9). The study clearly exhibited that nanocomposites material capacitance was enhanced in comparison with the PANI nanofibers, due to the synergistic effect between Fe_3O_4 nanoparticles and PANI nanofibers.

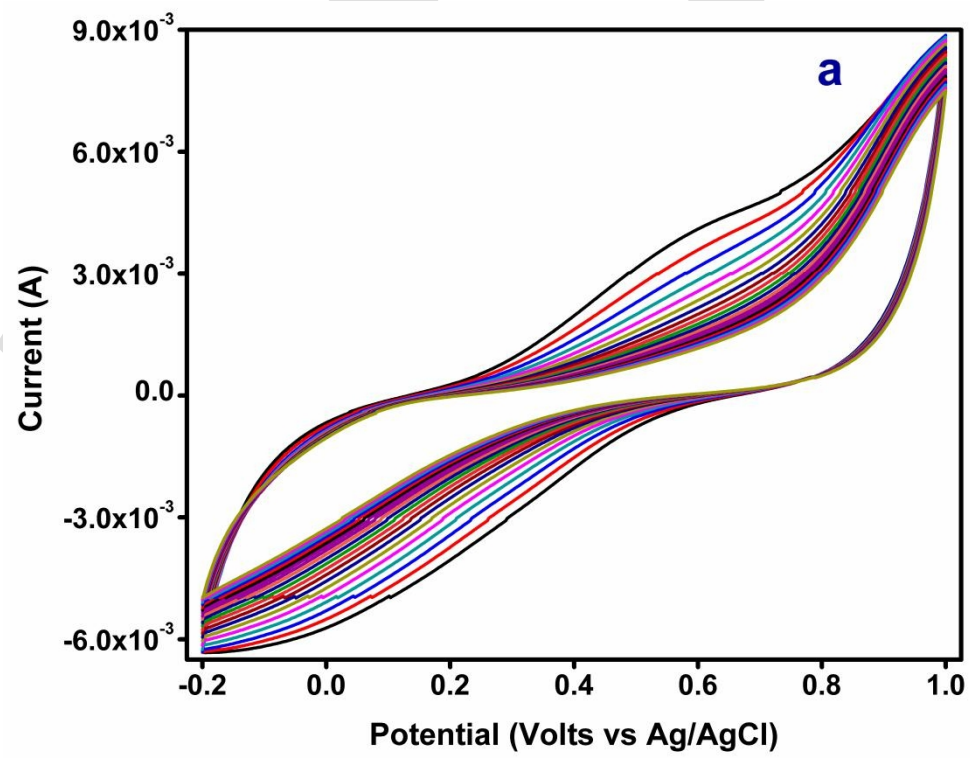

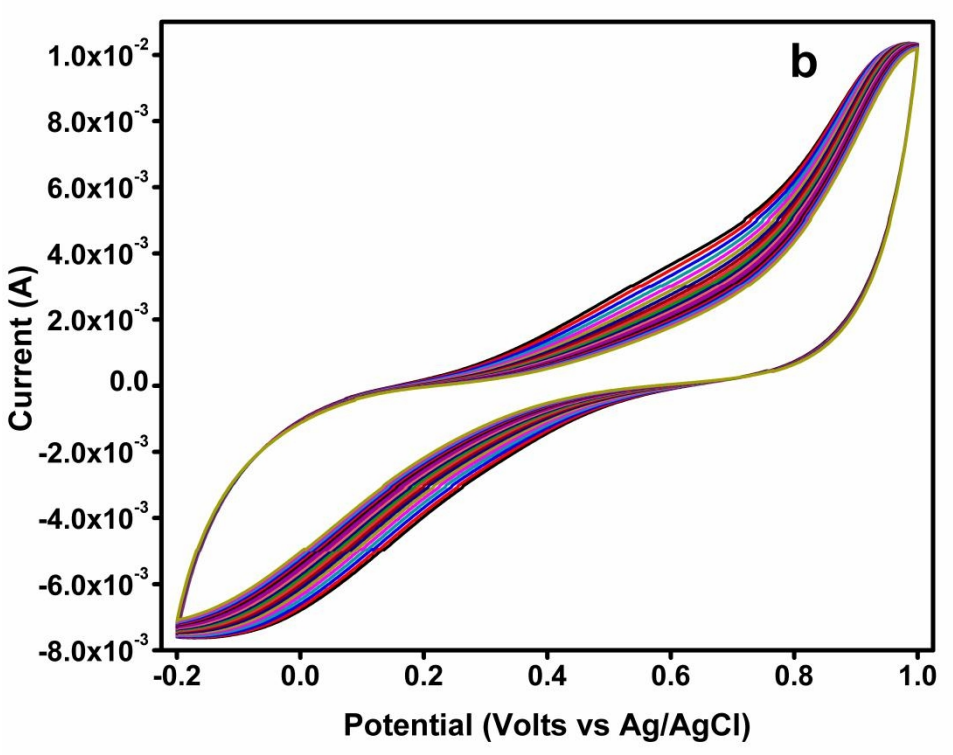

Fig. 10.CV curves of (a) PANI and (b) Fe_3O_4-PANI at 50 mV/s scan rate.

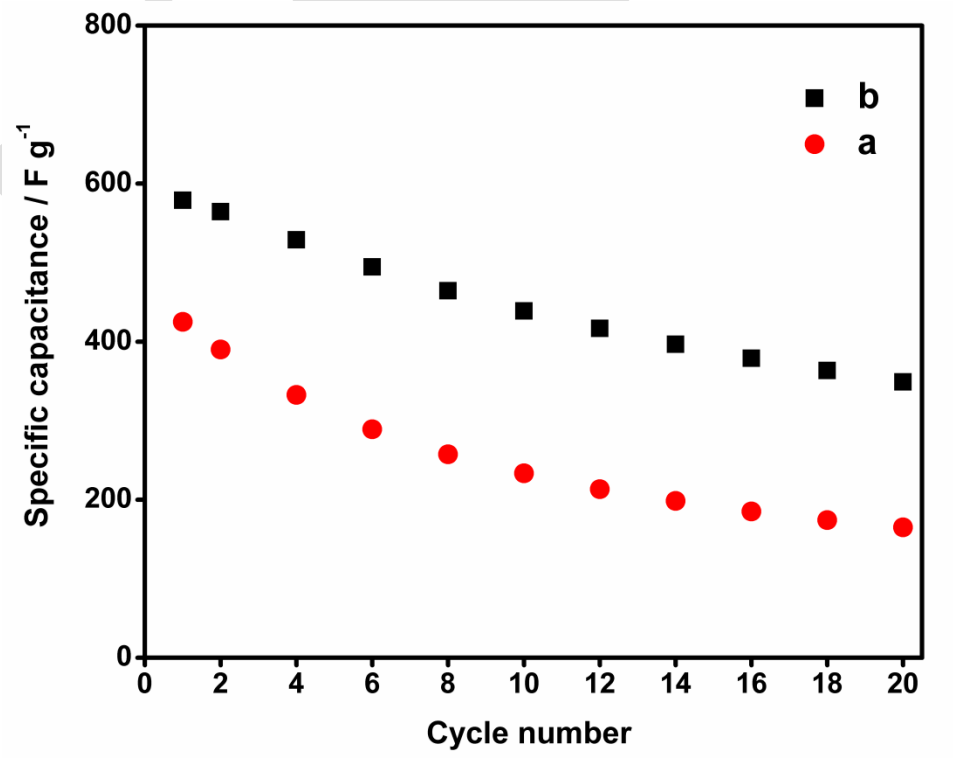

Fig. 11. Specific capacitance of PANI and Fe_3O_4-PANI sweep potential at 50 mV/s.

Fig. 10 shows the cyclic stability of PANI nanofibers and PANI-Fe_3O_4-PANI at the sweep rate of 50 mV/s for 20 cycles. Specific capacitance value was linearly decreasing for 10 cycles and subsequently the specific capacitance remained nearly constant (Fig. 11b). The specific capacitance of PANI nanofibers was 425 F/g in the first cycle and 165 F/g in the 20 cycles (Fig. 11a) clearly indicated that the Fe_3O_4 doped nanocomposites have high stability of the electrode material than PANI nanofibers for long cyclic life.

4. Conclusion

In the present work, we successfully synthesised the PANI and Fe_3O_4-PANI composite nanofibers using SLCs as soft templates. The synthesised Fe_3O_4-PANI nanocomposites were found to be concretely confinements due to the strong interaction between Fe_3O_4 nanoparticles on the surface of PANI nanofibers. The study revealed that conductive material PANI and Fe_3O_4-PANI nanofibers have plausible application as supercapacitor as they showed significant capacitance values of 629 F/g and 933 F/g, respectively.

Supplementary Information (SI)

Digital camera photographs are shown in supplementary information.

Acknowledgement

SYP grateful to DST-INSPIRE (IF-120468), New Delhi for providing financial support.

References

1. G. Surendran, L. Ramos, B. Pansu, E. Prouzet, P. Beaunier, F. Audonnet, H. Remita, Chem. Mater. 19 (2007) 5045.
2. S. Dutt, P. F. Siril, J. App. Poly. Sci. 131 (2014) 40801.
3. S. Dutt, P. F. Siril, Mat. Lett. 124 2014 50.
4. M. Nandi, R. Gangopadhyay, A. Bhaumik, Micro and Meso. Mate. 109 (2008) 239.
5. J. Huang, S. Virji, B. H. Weiller, R. B Kaner, J. Am. Chem. Soc. 125 (2003) 314.
6. J. Huang, R. B. Kaner, J. Am. Chem. Soc. 126 (2004) 851.
7. S. Virji, J. Huang, R. B. Kaner, B. H. Weiller, Nano lett. 4 (2004) 491.
8. Y. Wang, Z. Liu, B. Han, Z. Sun, Y. Huang, G. Yang, Langmuir. 21 (2005) 833
9. Y. Wang, L. Gai, W. Ma, H. Jiang, X. Peng, L. Zhao, Ind. & Eng. Chem. Res. 54 (2015) 2279.
10. L. Li, A. R. O. Raji, H. Fei, Y. Yang, E. L. Samuel, J. M. Tour, ACS Appl. Mate. & Inter. 5 (2013) 6622.
11. T. Yao, T. Cui, H. Wang, L. Xu, F. Cui, J. Wu Nanoscale. 6 (2014) 7666.
12. L. Gai, X. Han, Y. Hou, J. Chen, H. Jiang, X. Chen, Dalt. Trans. 42 (2013) 1820.
13. Q. Xiao, X. Tan, L. Ji, J. Xue, Synth Metals. 157 (2007) 784.
14. C. Cui, Y. Du, T. Li, X. Zheng, X. Wang, X. Han, P. Xu, J. Phy. Chem. B. 116 (2012) 9523.
15. S. Ghosh, H. Remita, L. Ramos, A. Dazzi, A. Deniset-Besseau, P. Beaunier, G. Fabrice, A. Pierre-Henri, B. Francois, S. Remita, New J. Chem. 38 (2014) 1106.
16. S. Dutt, P. F. Siril, V. Sharma, S. Periasamy, New J. Chem. 39 (2015) 902.
17. A. M. Kalekar, K. K. K. Sharma, A. Lehoux, F. Audonnet, H. Remita, A. Saha, G. K. Sharma, Langmuir. 29 (2013) 11431.

18. A. M. Kalekar, K. K. Sharma, N. M. Luwang, G. K. Sharma, RSC Advances (2016) DOI: 10.1039/C5RA23138H.
19. G. Surendran, M. S. Tokumoto, E. Pena dos Santos, H. Remita, L. Ramos, P. J. Kooyman, C. V. Santilli, C. Bourgaux, P. Dieudonne, E. Prouzet, Chem. Mate., 17 (2005) 1505.
20. A. R. Mahdavian, M. A. S. Mirrahimi, Chem. Eng. J. 159 (2010) 264.
21. W.Wang, Q. Hao, W. Lei, X. Xia, X. Wang, RSC Advances, 2 (2012) 10268.
22. L. F. Chen, X. D. Zhang, H. W. Liang, M. Kong, Q. F. Guan, P. Chen, W. Zhen-Yu, S. H. Yu, ACS Nano, 6 (2012) 7092.
23. V. Gupta, N. Miura, Mate. Lett. 60 (2006) 1466.

Figure S1. Digital camera photographs of (a) lamellar mesophase in Triton X-100 in presence of 4 mM ANI (b) lamellar mesophase doped with Fe_3O_4 nanoparticles. (c) The dark green color was observed which indicate polymerization of ANI. (d) Synthesis of Fe_3O_4-PANI nanocomposites in swollen liquid crystal.

Chemical Physics Letters 671 (2017) 147–153

Contents lists available at ScienceDirect

Chemical Physics Letters

journal homepage: www.elsevier.com/locate/cplett

Research paper

Synthesis of Ibuprofen intermediate using alcoholic silver nanoparticles and its kinetics: A greener approach towards drug synthesis

Sandeep J. Pawar [a], Shivkumar Y. Patil [a], Pramod P. Mahulikar [a], Vishvanath S. Zope [b,*]

[a] School of Chemical Sciences, North Maharashtra University, Jalgaon 425001, MS, India
[b] Department of Chemistry, Moolji Jaitha College, Jalgaon 425001, MS, India

ARTICLE INFO

Article history:
Received 18 November 2016
In final form 10 January 2017
Available online 17 January 2017

Keywords:
Silver nanoparticles
Catalytic activity
E-factor
Recyclability
Ibuprofen
1-(4-isobutylphenyl)ethanol

ABSTRACT

Silver nanoparticles (AgNPs) were prepared and tested for the activity in the catalytic reduction of 4-nitrophenol to 4-aminophenol showing to be exceptionally active. Further, using AgNPs we catalytically synthesized 1-(4-isobutylphenyl)ethanol which is important drug intermediate for the widely used Ibuprofen. The rate constants were determined at temperatures 298 K, 303 K, 308 K, 313 K, 318 K, 232 K correspond to 0.29 min^{-1}, 0.37 min^{-1}, 0.40 min^{-1}, 0.43 min^{-1}, 0.50 min^{-1}, 0.68 min^{-1}, respectively. The activation energy of AgNPs is 23.25 kJ/mol. The number of collisions of reactants in the term of frequency factor was found to be high 1.99×10^8 min^{-1} and average heat of reaction is 26.1 kJ/mol. The recyclability study of AgNPs in the reduction of 1-(4-isobutylphenyl)ethanone (4-IBPEON) to 1-(4-isobutylphenyl)ethanol (4-IBPE) in six consecutive reaction cycles found to be (0.91 g, 90%), (0.89 g, 88%), (0.87 g, 86%), (0.84 g, 83%), (0.84 g, 83%), (0.81 g, 80%), respectively. We promisingly minimize the waste generated in the synthesis of 4-IBPE by calculation E-factor and atom efficiency and was found to 0.57 and 81.56%, respectively. Reported experimental results were directly relevance to develop theoretical concepts.

1. Introduction

In the era of nanoscience and nanotechnology [1], nanostructured material have played an important role in the catalytic synthesis of pharmaceutical drugs due to their high surface area, small particle size as well as "*nano-effect*" [2] originating from small size. Currently, a need to develop nanostructured materials based reduction methods for the synthesis of pharmaceutical drugs on industrial process is highly essential in order to minimize waste, and improve E-factors and atom efficiency [3]. This trend toward the green chemistry, to set high yield of product and environmentally benign processes that ascribes the economic value to eliminating waste. Noble metal nanoparticles (NPs) is of fundamental importance to the pharmaceutical, chemical, dyes and pesticides industries [4,5]. Amongst the NPs, silver nanoparticles (AgNPs) increasing interest towards the better catalytic performance because of cheap and attractive physiochemical properties. AgNPs, amongst other applications, has also been presently exploited as a catalyst in heterogeneous catalysis reactions [6]. For the synthesis of AgNPs variety of methods have been reported including chemical reduction method in aqueous solutions [7] or non-aqueous solutions [8], template method [9], electrochemical or sonochemical reduction method [10], photocatalytic or photoinduced reduction method [11], microwave assisted synthesis [12], irradiation reduction method [13], microemulsion method [14] biochemical reduction method [15] and many more. Foremost chemical reduction method in aqueous solution is the most conventional, clean and safe method. The uncapped AgNPs were commonly synthesized by chemical reduction method [16]. AgNPs have been widely used as catalyst in the model reaction of reduction of 4-nitrophenol (4-NP) to 4-aminophenol (4-AP) by using $NaBH_4$ [17]. The catalytic reduction of 4-NP was monitored by UV–Vis spectrophotometer under the mild reaction condition in aqueous medium.

Further, 1-(4-isobutylphenyl)ethanol (4-IBPE) is the most important drug intermediate for the synthesis of Ibuprofen, a well-known non-steroidal anti-inflammatory drug (NSAID). We efficiently overcome, the use of hazardous organic solvents [18] reported so far in the synthesis of 4-IBPE from 1-(4-isobutylphenyl)ethanone (4-IBPEON) using aqueous ethanol which resulted in high yield of product. The E-factor (Environmental Factor) and atom efficiency (atom Utilization) are most important phenomenon towards greener and environmental benign synthesis [19–21]. The E-Factor is the most important concept played a major role in chemical industry, particularly in pharmaceutical industry, on the problem on waste generation in chemical manufacture. E-Factor is defined as the mass ratio of waste to desired product and the atom efficiency. Atom efficiency is the

* Corresponding author.
E-mail address: vszope2@gmail.com (V.S. Zope).

http://dx.doi.org/10.1016/j.cplett.2017.01.021
0009-2614/

ratio of the molecular weight of the desired product to the sum of the molecular weights of all materials produced in the process [19–21].

In present investigation we have reported for the first time conventional catalytic synthesis of 4-IBPE from 4-IBPEON by using sodium borohydride ($NaBH_4$) in the presence of AgNPs in aqueous ethanol (Scheme 1).

The reaction was achieved successfully in six consecutive cycles of catalyst and completed within 5–10 min with high yield of product. Also, we have been promisingly reported the kinetics of AgNPs which are helpful to material chemistry researchers.

2. Experimental

2.1. Chemicals

All chemicals (4-nitrophenol ($C_6H_5NO_3$, 99%), sodium borohydride ($NaBH_4$, 99%), silver nitrate, ($AgNO_3$, 99.9%) 1-(4-isobutylphenyl)ethanone ($C_{12}H_{16}O$, 98%) and deionized water from Milli-Q system) were purchased from Sigma-Aldrich or Spectrochem or HiMedia and used as received.

2.2. Characterizations

The characterizations of AgNPs were collected from various instrumental techniques. The UV–Visible absorption measurement was performed on Shimadzu UV1800 Spectrophotometer. Water as blank and reference. Transmission electron microscopy was performed on a Philips CM-200 TEM operating at 200 kV, by depositing 20 μL of dispersed sample onto a 300 mesh copper grid coated with carbon layer. IR spectra were collected at room temperature from Shimadzu FTIR-Affinity-1instrument in dried KBr pellets in the range 4000–400 cm^{-1}. The ^1H NMR spectra at 400 MHz and ^{13}C NMR spectra at 100 MHz were collected from BRUKER AVANCE II Spectrometer using DMSO-d_6 as solvent and tetramethylsilane ($SiMe_4$) as internal standard. Mass spectra (MS) of 1-(4-isobutylphenyl)ethanol was collected from WATERS, Q-TOF MICROMASS (LC-MS) instrument.

2.3. Synthesis of silver nanoparticles (AgNPs)

The AgNPs were synthesized by using chemical reduction method. In brief, 10 mL of 1×10^{-3} M $AgNO_3$ taken in 50 ml of beaker and kept on magnetic stirrer. Then freshly prepared ice cold 30 mL solution of 2×10^{-3} M $NaBH_4$ was hastily added into $AgNO_3$ with vigorous stirring in which the colour change from black to orange and finally pale yellow was observed. Then AgNPs solution was stirred for six hours for good stability and prepared nano-size of AgNPs particles. Finally, prepared AgNPs were kept overnight to remove excess hydrogen and used as a catalyst in the model after their characterization.

2.4. Typical procedure for catalytic reduction of 4-nitrophenol (4-NP)

The heterogeneous catalytic reduction of 4-NP was performed at room temperature in air. In this typical reaction 1.0 mL of 5×10^{-2} M $NaBH_4$ and 10 μL of AgNPs were mixed for two minutes in 3.0 mL quartz cuvette. To this mixture 1.5 mL of 1×10^{-4} M PNP was added and mixed. The reaction was followed by observing the absorbance spectrum of 4-NP at λ 400 nm. The 4-NP spectrum diminished at every one minute time interval and new spectrum was observed at λ 300 nm is indicates that formation of new product, which was confirmed by isosbestic points [22]. This results were in good agreements with reported literatures [23]. The absorbance spectra were recorded within the wavelength range of 250–600 nm. Further, the same experiment were also performed in the temperature range of 298–323 K to determine the effect of temperature on the Pseudo first-order rate constant.

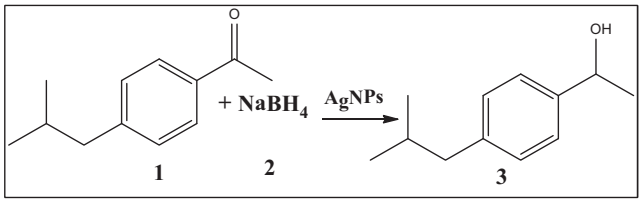

Scheme 1. Synthesis of 4-IBPE from 4-IBPEON in the presence of AgNPs.

2.5. Synthesis of 1-(4-isobutylphenyl)ethanol (4-IBPE)

Aqueous ethanol (4.0 mL) was added in 3.0 mL of AgNPs in round bottom flask, kept in ice bath with constant stirring. This mixture we named as "*Alcoholic AgNPs*". In the mixture 0.43 g of $NaBH_4$ was slowly added and finally 1.0 g. of 4-IBPEON added with constant stirring. After complete addition, the reaction mixture was removed from the ice bath and stirring was continued at room temperature. The reaction was completed within 5–10 min and it was preliminary confirmed by thin layer chromatography (TLC). The product was isolated using ethyl acetate as organic layer and AgNPs remained in alcoholic layer. The solvent was removed by rotary evaporator and product was dried at room temperature.

2.6. Recycling studies

The recycling study of AgNPs were reported so far, for the catalytic reduction of 4-NP to 4-AP. The above (4-NP to 4-AP) recycling confines towards, used concentration of reactant was low, the reaction was monitor by UV–Vis spectrophotometer. For the first time we have performed the recycling study of AgNPs in the reduction of 4-IBPEON to 4-IBPE. In detail, as discussed above (**2.5**), we synthesized 4-IBPE in first cycle. In second cycle in alcoholic liquor containing AgNPs was added 1.0 g of IBPEON and 0.43 g of $NaBH_4$ with constant stirring at room temperature. After completion of reaction, the product was isolated from ethyl acetate as organic layer and AgNPs remained in alcoholic layer. Finally the solvent from the product was removed by rotary evaporator. Repeated the similar procedure for next consecutive reaction cycles and recorded the percent yield of product in every cycles. We conclude that the AgNPs showed good catalytic activity against poisoning of catalyst after six consecutive reaction cycles.

2.7. Reaction mechanism

In the mechanism of reduction reaction of 4-IBPEON to 4-IBPE involves the initial adsorption of 4-IBPEON and BH_4^- ions on the catalyst surface. Due to the close vicinity of the reacting groups on the catalyst surface, the reduction becomes practicable. The catalyst provide surface and helps this reduction process by relaying hydride ion to from BH_4^- ions to the 4-IBPEON to forms 1-(4-isobutylphenyl)ethanoate ion. This ion absorbs proton solvent and finally forms 4-IBPE.

3. Results and discussion

3.1. UV–Vis. Spectrometry of silver nanoparticles (AgNPs)

The synthesized AgNPs by chemical reduction method were confirmed by UV–Vis Spectrophotometer that showed the narrow surface plasmon resonance (SPR) band at 405 nm. (Fig. 1). Two different SPR were observed for AgNPs, and alcoholic AgNPs. The

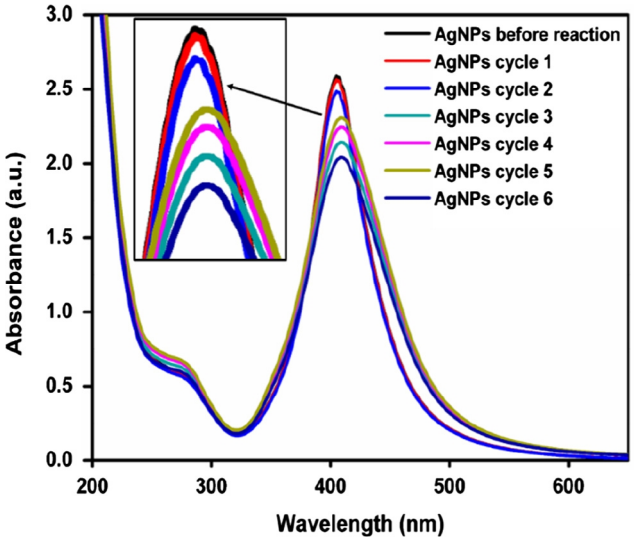

Fig. 1. UV. Vis SPR of AgNPs, black SPR before reaction and blue SPR (cycle 6) after reaction.

black SPR was recorded before proceeding the reaction while blue SPR was recorded after completion of all reaction cycles (after cycle 6). The broad peaks showed in inset of Fig. 1. After completion of every reaction cycle UV–Vis spectra was recorded. We observed that decrease in SPR of alcoholic AgNPs was due to the dilution of AgNPs by addition of reactants in every reaction cycle.

3.2. Morphology of silver nanoparticles (AgNPs)

The morphological study using TEM of synthesized AgNPs was carried out (Fig. 2, panel a, b). It was observed that the spherical shaped rigid particles having a narrow size distribution showed good catalytic activity and high surface area. The particles were uniform and distinctly present in aqueous collide solution. There was no change found in morphology of AgNPs by adding alcohol (Fig. 2, panel c). It proved that the TEM image of alcoholic AgNPs is in agreements with AgNPs and thus, it confirmed that the AgNPs showed good stability after six consecutive reaction cycles. The average particle size of AgNPs (12 ± 0.84 nm) (Fig. 2. Panel d) was confirmed by TEM image.

3.3. Kinetics and catalytic activity of silver nanoparticles (AgNPs)

The kinetics study was performed by using Langmuir-Hinshelwood mechanism [22]. Assuming that 4-NP and $NaBH_4$ adsorbed on the surface of AgNPs, the interaction of $NaBH_4$ on the surface of AgNPs took place and which ultimately led to the liberation of hydrogen and 4-NP was converted to 4-AP. In general, the rate law for 4-NP reduction by $NaBH_4$ is given by Eq. (1),

$$-\frac{d[4NP]}{dt} = k[4NP]^a[BH_4^-]^b \quad (1)$$

In Eq. (1) k is the pseudo-first order rate constant, calculated from Langmuir-Hinshelwood equation given by Eq. (2).

$$\ln\frac{C_0}{C} = kt \quad (2)$$

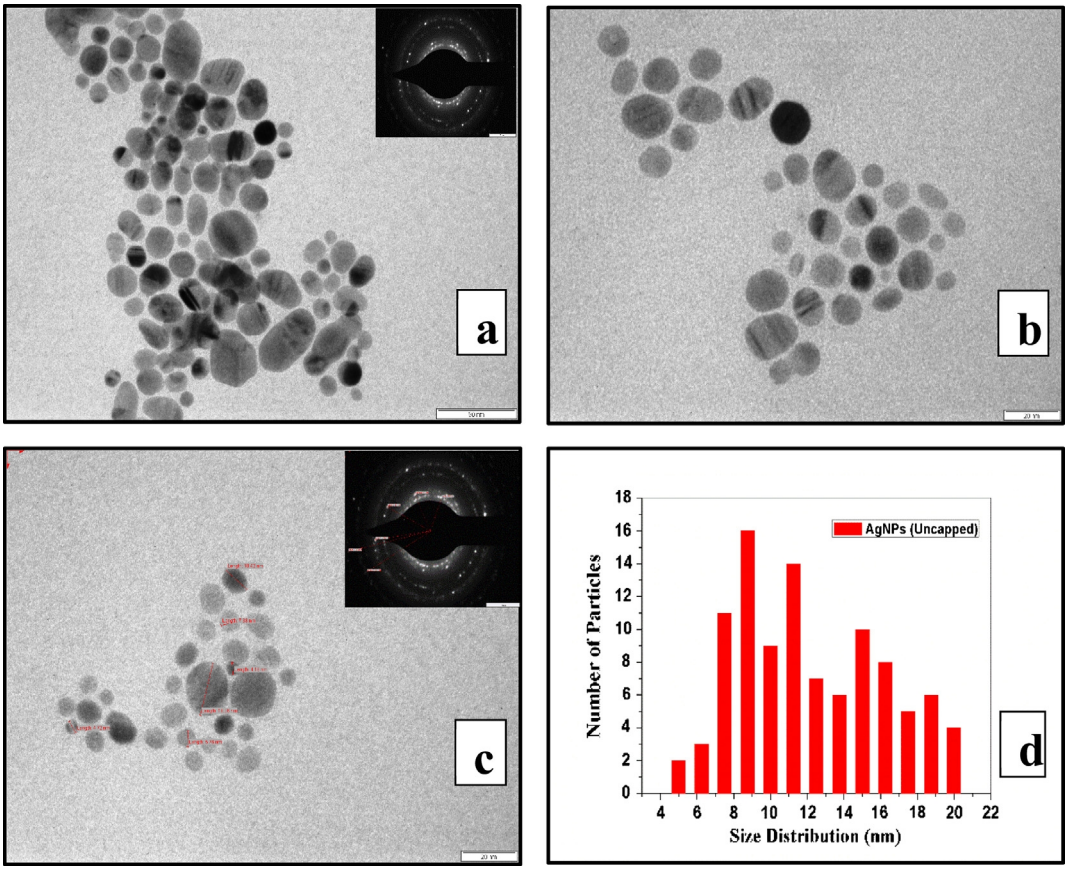

Fig. 2. TEM image of AgNPs (panel a, b) and alcoholic AgNPs (panel c); panel (a) and (c), inset is the selected area electron diffraction (SAED) pattern. (d) Particle size of AgNPs showing average size is about 12 ± 0.84 nm approx.

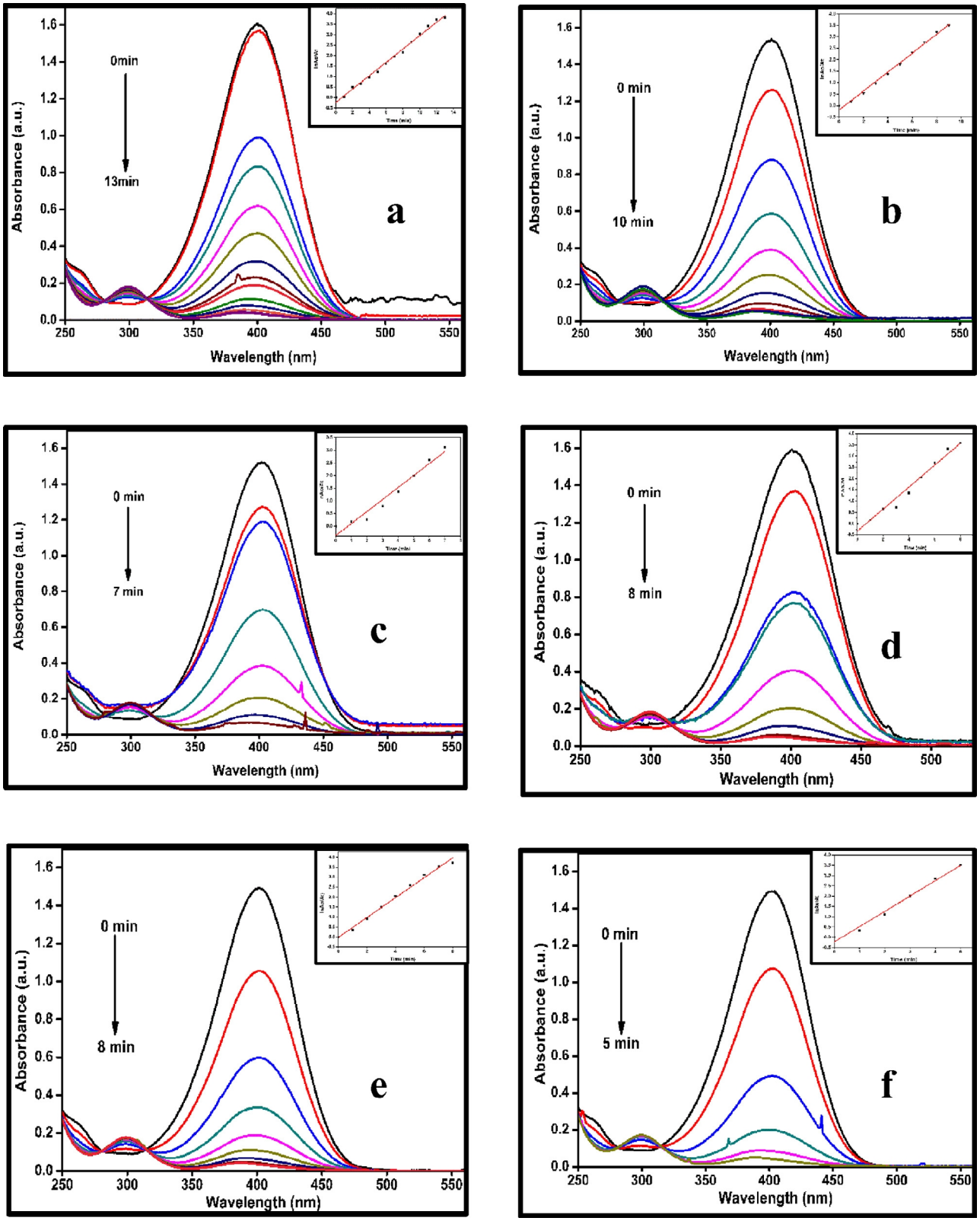

Fig. 3. The UV–Vis plots of absorbance as a function of wavelength at temperature a 298 K; b 303 K; c 308 K; d 313 K; e 318 K; f 323 K for regular time intervals indicates the disappearance of peak of 4-NP due to the catalytic reduction of 4-NP to 4-AP by using $NaBH_4$ in presence of AgNPs; in inset of each panel shows corresponding linear plots of ln (A_0/At) versus time. Reaction conditions: [4-NP] = 1×10^{-4} M; [$NaBH_4$] = 5×10^{-2} M; [AgNPs] = 2.5×10^{-4} M.

In Eq. (2), C_0 and C are the initial and final concentrations having equivalent in terms of (A_0 and A_t respectively) monitor at fixed wavelength at time t, k is the pseudo-first order rate constant for AgNPs. Hence, for the constant catalyst concentration, a plot of ln (A_0/At) with respect to time gives straight line whose slope is the k. The k also determined at various temperatures ranging from

298 to 323 K and activation energy (Ea) of the catalytic reduction of 4-NP to 4-AP by using AgNPs was calculated by Eq. (3).

$$k = Ae^{-Ea/RT} \quad (3)$$

In Eq. (3), k is the pseudo-first order rate constant at temperature T, A is the frequency factor, Ea is the activation energy, R is the universal gas constant ($8.314\ J\ K^{-1}\ mol^{-1}$) In the catalytic reduction of 4-NP to 4-AP by using $NaBH_4$ in the presence of AgNPs the heat of reaction ΔH for the solution phase reaction is calculated from Eq. (4).

$$\Delta H = Ea + RT \quad (4)$$

In order to study the effect of temperature on the pseudo-first order rate constant, (Fig. 3.) the reactions were also performed in the temperature range of 298–323 K. The temperature of the solution in the quartz cuvette was controlled by water circulated peltier unit with an accuracy of temperature ±0.3 °C inside the cuvette holder.

Fig. 3(Panel a–f) Illustrate that as the temperature increases in the range of 298–323 K for the reduction of 4-NP rate of the reaction also increased. *i.e.* temperature is directly proportional to rate of reaction. At the temperature 298 K, 4-NP reduced within 13 min for the AgNPs catalyzed reaction at 400 nm. Similarly for different temperatures 303 K, 308 K, 313 K, 318 K and 323 K, reduced in 10, 7, 8, 8 and 5 min, respectively. Finally, we conclude that pseudo-first order kinetics was observed at all temperatures and delay of time is reduced with increasing temperature [24–26]. (See ESI Fig. S1, a) The pseudo-first order rate constants were determined by plotting $\ln(A_0/At)$ as a function of time. (Fig. 3, insets a, b, c, d, e and f). To know the heterogeneous catalytic mechanism of AgNPs in the reduction of 4-NP to 4-AP, the pseudo-first order rate constants were also determined at temperature ranging from 298 K to 323 K. The calculated rate constants with respect to temperatures 298 K, 303 K, 308 K, 313 K, 318 K and 323 K were found to be $0.29\ S^{-1}$, $0.37\ S^{-1}$, $0.40\ S^{-1}$, $0.43\ S^{-1}$, $0.5\ S^{-1}$ and $0.68\ S^{-1}$, respectively. From this investigation the rate constants were increased as temperature increased and also strictly follows pseudo-first order kinetics (Table 1.).Activation energy of metal nanostructures likely depends on the size and shape of nanoparticles [27]. For the determination of activation energy of the reaction, temperature dependent study were performed from 298 K to 323 K for AgNPs catalyzed reduction of PNP to PAP (see ESI, Fig. S1, a) and the pseudo-first order rate constants for AgNPs were fitted using Arrhenius equation (Eq. (3)) and the activation energy was calculated using the slope of the linear plot of ln (k) versus 1000/T (see ESI, Fig. S1 panel b). The calculated activation energy for AgNPs was found to be 23.58 kJ/mol. The activation energy calculated for the AgNPs catalyzed conversion of 4-NP to 4-AP in this study is lowest so far, while the lowest activation energies 33.8–45 kJ/mol has been reported for AgNPs and AgNPs supported different agents or composites [27–30]. From the Arrhenius equation frequency factor was determined and found to very high 1.99×10^8 per min. (Eq. (3)). Higher the frequency factor proved more number of collisions of reactants. The average heat of reaction for the reduction of 4-NP to 4-AP was found to 26.1 kJ/mol. (Eq. (4)). E-factor and Atom efficiency (atom utilization) are the most important concept for metal catalyzed reactions towards the environmental benign synthesis. In the present investigation the concept E-factor and atom efficiency were studied for AgNPs catalyzed reduction of 4-IBPEON to 4-IBPE (Scheme 2). E-factor was found to 0.57 and proved that very minimum of waste was generated in the synthesis of 4-IBPE. Also, the atom efficiency was found to 81.56% and proved that higher number of atom involved in the formation of product 4-IBPE.

Table 1, shows the kinetic evaluation of AgNPs, the rate constant was found to be steadily increasing with temperature. At temperature 298 K, 4-NP reduced in 13 min while at 323 K 4-NP reduced within 5 min, is also proves that the AgNPs were stable at temperature 323 K and reduced fastly due to the rigidity of nanoparticles reported in TEM images. The activation energy (23.58 kJ/mol) was also lowered and frequency factor was found to be very highest (1.99×10^8), which concluded that higher the collisions of reactants in solution on the surface of AgNPs due to small particle size of AgNPs provide high surface area and lower the activation energy and increase the rate constant with respec-

Table 1
The rate constants (k), at different temperatures, the activation energy (Ea), frequency factor (A) and average heat of reaction for AgNPs catalyzed reduction of 4-NP to 4-AP by using $NaBH_4$.

	Temperature T/(K)	Rate constant k/min^{-1}	Activation energy (Ea)/kJ/mol	Frequency factor A/min	Average heat of reaction ΔH/kJ/mol
AgNPs	298	0.29 ± 0.04	23.58	1.99×10^8	26.1
	303	0.37 ± 0.03			
	308	0.40 ± 0.01			
	313	0.43 ± 0.01			
	318	0.50 ± 0.01			
	323	0.68 ± 0.03			

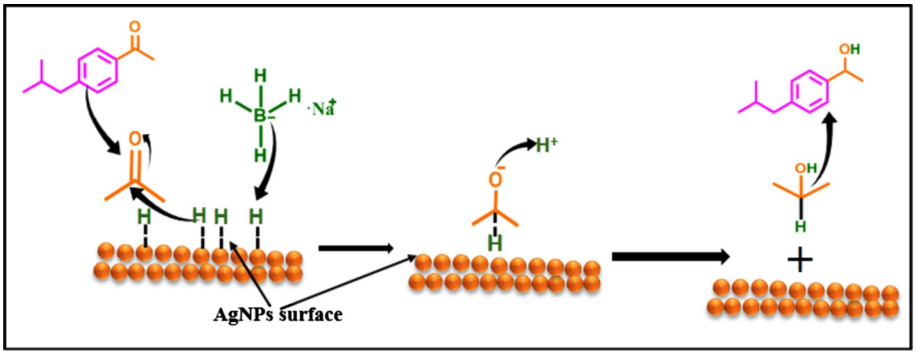

Scheme 2. Reaction mechanism: reduction of 4-IBPEON to 4-IBPE in the presence of AgNPs.

Table 2
The comparison of AgNPs with different stabilizing agent or supporting agents, size, rate constant, activation energy, frequency factor and heat of reaction.

Nanoparticles	Size of nanostructures/nm	Rate constant k/min^{-1}	Activation energy (Ea)/kJ/mol	Frequency factor A/min	Heat of reaction ΔH/kJ/mol
AgGME [30]	25	ND	41.00	ND	ND
AgDENs [31]	3.37 ± 0.6	0.0001	45.7	ND	34 ± 2.7
AgNPs [32]	ND	ND	35.16	ND	ND
AgNPs[#]	7–13	0.37	23.58	1.99×10^8	26.1

[*] ND = Not Determined.
[#] =In this work.

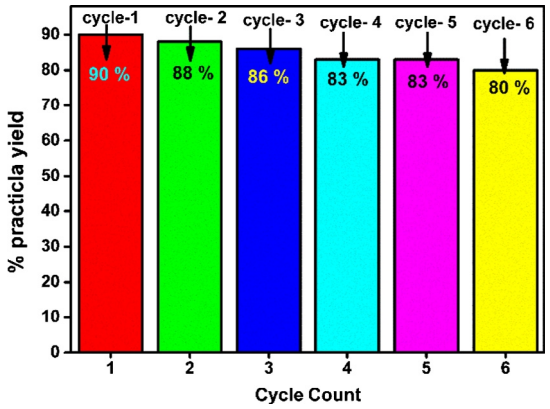

Fig. 4. Percent practical yield of 4-IBPE against number of cycle count.

tive to temperature. Finally, the heat of reaction at different temperatures was calculated and the average of heat of reaction was found to be 26.1 kJ/mol.

In the comparative study of AgNPs (Table 2), we found the lowest activation energy with high frequency factor and lower heat of reaction because of high catalytic activity of AgNPs.

3.4. Yield and characterization of 1-(4-isobutylphenyl)ethanol (4-IBPE)

We have been demonstrated catalytic reduction of 4-IBPEON to 4-IBPE by using $NaBH_4$ in the presence of AgNPs dispersed in dilute alcohol is in the interest of well-known model reaction for the catalytic reduction of 4-NP to 4-AP. The stability of catalyst have been studied by recycling and found to be stable to six successive cycles in laboratory scale. The reaction was practically conducted on laboratory scale in the laboratory by with 1.0 gm of 4-IBPEON and 3 mL of AgNPs and preliminary monitored by thin layer chromatography (TLC) and melting point. The yield of the 4-IBPE was slightly decreased with respect to recycling cycles and found to be (0.91 g, 90%), (0.89 g, 88%), (0.87 g, 86%), (0.84 g, 83%), (0.84 g, 83%) and (0.81 g, 80%) with respect to cycles 1 to 6, respectively (Fig. 4).

Lastly, the synthesized 4-IBPE was characterized by using FTIR, ^{1}H NMR, ^{13}CMR and mass spectroscopy (For spectra see SI, Figs. S2, S3, S4 and S5). The characterization data of 4IBPE as given below.

Spectral data of 3. 1-(4isobutyl)phenyl ethanol (IBPE) is isolated as viscous oil; b.p. 245–246 °C; FT-IR (KBr) cm^{-1}: 3336 (OH), 2954–2899 (CH); 1666–1624 (C—C═C), ^{1}H NMR (400 MHz, $CDCl_3$,) δ_H: 0.88 (6H, d, J = 6.6 Hz); 1.40 (3H, d, J = 6.4 Hz), 1.83 (1H, m, CH), 2.43 (2H, d, J = 7.1 Hz CH_2), 2.71 (1H, br s, OH), 4.76 (1H, q, J = 6.4 Hz CH), 7.07 (2H, d, J = 8.08 Hz, Ar—H), 7.21 (2H, d, J = 8 Hz, Ar—H), ^{13}C NMR (400 MHz, $CDCl_3$,) δc: 22.5, 25.1, 30.3, 45.2, 70.0, 125.3, 129.1, 140.7, 143.3; ESI-MS: m/z = 177.13 [M - H]$^+$, 161.09 [M-OH] The result were found to be well agreement with the reported literatures to conform the product 4-IBPE.

4. Conclusion

In summary, we have efficiently investigated the catalytic performance of AgNPs in the reduction of 4-NP to 4-AP by using $NaBH_4$. In the UV– Vis spectra observed isosbestic points, recyclability of catalyst and kinetics all have to be accounted by keeping an eye on to the published mechanism. The recyclability study of AgNPs has been reported for the first time and investigated in the reduction of 4-IBPEON – 4-IBPE by using $NaBH_4$ in "*Alcoholic AgNPs*" and found to be in the range of very excellent to good with better yield of 4-IBPE in each stage of total six cycles. This work useful to study the stability of AgNPs which are withstand in the organic reaction conditions to improve the catalytic recycling and efficiency for many applications. We also successfully determined E-factor and atom efficiency, were proved minimization of waste generated. The costly and important drug intermediate of Ibuprofen, 4-IBPE was economically synthesized in the laboratory by environmentally benign process. In future, attempts will made to scale up the synthesis of 4-IBPE in pilot plant by collaboration with pharmaceutical industry. This results of the present investigation could be helpful for material chemistry scientists as well as organic researches to design the safer synthesis of important commonly used pharmaceutical drugs.

Acknowledgements

The authors would like to thank BSR-UGC, New Delhi for financial support. In addition SAIF, Chandigarh, Punjab University for Spectroscopy characterizations, SAIF, IIT Bombay for TEM characterization.

Appendix A. Supplementary material

Supplementary data associated with this article can be found, in the online version, at http://dx.doi.org/10.1016/j.cplett.2017.01.021.

References

[1] J. Schummer, Scientometrics 59 (3) (2004) 425–465.
[2] Y. Xu, L. Chen, X. Wang, W. Yao, Q. Zhang, Nanoscale 7 (24) (2015) 10559–10583.
[3] R.A. Sheldon, Pure Appl. Chem. 72 (7) (2000) 1233–1246.
[4] W.J. Stark, P.R. Stoessel, W. Wohlleben, A. Hafner, Chem. Soc. Rev. 44 (16) (2015) 5793–5805.
[5] K. Philippot, P. Serp, Nanomaterials in Catalysis, first ed., WILEY-VCH Verlag GmbH and Co. KGaA, Weinheim, 2013.
[6] D. Astruc (Ed.), Nanoparticles and Catalysis, vol. 1, Wiley-VCH, Weinheim, 2008.
[7] N. Leopold, B. Lendl, J. Phys. Chem. B 107 (24) (2003) 5723–5727.
[8] I. Pastoriza-Santos, L.M. Liz-Marzan, Nano Lett. 2 (8) (2002) 903–905.
[9] S.H. Chen, D.L. Carroll, Nano Lett. 2 (9) (2002) 1003–1007.
[10] C. Johans, J. Clohessy, S. Fantini, K. Kontturi, V.J. Cunnane, Electrochem. Commun. 4 (3) (2002) 227–230.
[11] Q.F. Zhou, Z. Xu, J. Mater. Sci. 39 (7) (2004) 2487–2491.
[12] S. Komarneni, D.S. Li, B. Newalkar, H. Katsuki, A.S. Bhalla, Langmuir 18 (15) (2002) 5959–5962.
[13] S.H. Choi, S.H. Lee, Y.M. Hwang, K.P. Lee, H.D. Kang, Radiat. Phys. Chem. 67 (3) (2003) 517–521.

[14] X.W. Zheng, L.Y. Zhu, X.J. Wang, A.H. Yan, Y. Xie, J. Cryst. Growth 260 (1) (2004) 255–262.
[15] J.L. Gardea-Torresdey, E. Gomez, J.R. Peralta-Videa, J.G. Parsons, H. Troiani, M. Jose- Yacaman, Langmuir 19 (4) (2003) 1357–1361.
[16] T. Zidki, H. Cohen, D. Meyerstein, Phys. Chem. Chem. Phys. 8 (30) (2006) 3552–3556.
[17] P. Herves, M. Perez-Lorenzo, L.M. Liz-Marzan, J. Dzubiella, Y. Lu, M. Ballauff, Chem. Soc. Rev. 41 (17) (2012) 5577–5587.
[18] M. Poliakoff, P. Licence, Nature 450 (7171) (2007) 810–812.
[19] R.A. Sheldon, J. Chem. Tech. Biotechnol. 68 (1997) 381–388.
[20] R.A. Sheldon, Chem. Commun. 29 (2008) 3352–3365.
[21] R.A. Sheldon, Green Chem. 9 (2007) 1273–1283.
[22] T. Aditya, A. Pal, T. Pal, Chem. Commun. 51 (46) (2015) 9410–9431.
[23] L. Ai, H. Yue, J. Jiang, J. Mater. Chem. 22 (44) (2012) 23447–23453.
[24] Y. Mei, G. Sharma, Y. Lu, M. Ballauff, Langmuir 21 (2005) 12229–12234.
[25] Y. Lu, Y. Mei, M. Drechsler, T. Irrgang, R. Kempe, M. Ballauff, J. Phys. Chem. B 21 (26) (2005) 12229–12234.
[26] Y. Lu, Y. Mei, R. Walker, M. Ballauff, M. Drechsler, Polymer 47 (2006) 4985–4995.
[27] S. Panigrahi, S. Basu, S. Praharaj, S. Pande, S. Jana, A. Pal, S.K. Ghosh, T. Pal, J. Phys. Chem. C 111 (2007) 4596–4605.
[28] S. Butuna, N. Sahiner, Polymer 52 (11) (2011) 4834–4840.
[29] K.S. Shin, J.Y. Choi, C.S. Park, H.J. Jang, K. Kim, Catal. Lett. 133 (1–2) (2009) 1–7.
[30] N. Pradhan, A. Pal, T. Pal, Colloids Surf. A Physicochem. Eng. Asp. 196 (2) (2002) 247–257.
[31] M. Nemanashi, R. Meijboom, J. Colloid Interf. Sci. 389 (1) (2013) 260–267.
[32] W. Gan, B. Xu, H.L. Dai, Angew. Chem. Int. Ed. 50 (29) (2011) 6622–6625.